Carbonation in Low-Temperature CO_2 Electrolyzers: Causes, Consequences, and Solutions

Mahinder Ramdin,* Othonas A. Moultos, Leo J. P. van den Broeke, Prasad Gonugunta, Peyman Taheri, and Thijs J. H. Vlugt

Read Online

ACCESS | Metrics & More | Article Recommendations

ABSTRACT: Electrochemical reduction of carbon dioxide (CO_2) to useful products is an emerging power-to-X concept, which aims to produce chemicals and fuels with renewable electricity instead of fossil fuels. Depending on the catalyst, a range of chemicals can be produced from CO_2 electrolysis at industrial-scale current densities, high Faraday efficiencies, and relatively low cell voltages. One of the main challenges for up-scaling the process is related to (bi)carbonate formation (carbonation), which is a consequence of performing the reaction in alkaline media to suppress the competing hydrogen evolution reaction. The parasitic reactions of CO_2 with the alkaline electrolytes result in (bi)carbonate precipitation and flooding in gas diffusion electrodes, CO_2 crossover to the anode, low carbon utilization efficiencies, electrolyte carbonation, pH-drift in time, and additional cost for CO_2 and electrolyte recycling. We present a critical review of the causes, consequences, and possible solutions for the carbonation effect in CO_2 electrolyzers. The mechanism of (bi)carbonate crossover in different cell configurations, its effect on the overall process design, and the economics of CO_2 and electrolyte recovery are presented. The aim is to provide a better understanding of the (bi)carbonate problem and guide research directions to overcome the challenges related to low-temperature CO_2 electrolysis in alkaline media.
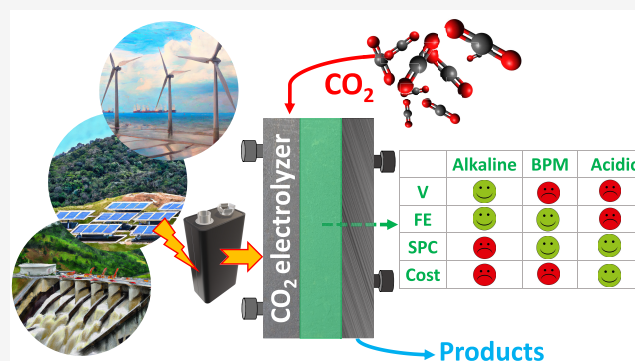
1. INTRODUCTION

Electrochemical reduction of CO_2 (CO2R) to value-added products is an element of carbon capture and utilization (CCU), which has been identified as a complementary measure to reduce CO_2 emissions.[1] The past decade, a significant effort has been made to improve the performance metrics of the electrochemical CO2R process.[2−5] By using gas diffusion electrodes (GDEs), optimized catalyst and reaction conditions, and proper reactor engineering, we are able to obtain several CO2R products at industrial-scale current densities (CDs), high Faraday efficiencies (FEs), low cell voltages, and extended durability/stability.[6−10] The high-temperature solid oxide electrolysis cell (SOEC) for CO_2 reduction to carbon monoxide (CO) is commercialized by Haldor Topsoe,[11] while Sunfire[12] and others are currently bringing the co-SOEC process for syngas production to the market. In sharp contrast, the low-temperature CO_2 electrolysis process is suffering from a major drawback, which is related to the carbonation of the electrolyte as a consequence of performing CO2R in alkaline conditions to suppress the hydrogen evolution reaction (HER). The CO2R reaction (CO2RR) produces hydroxide ions at the cathode electrode/electrolyte interface that can react with fresh

supplied CO_2 to form (bi)carbonates. Note that, for an aqueous CO_2 system, there is an equilibrium between carbonic acid, bicarbonate, and carbonate, where the distribution of the species is governed by the pH. Here, with (bi)carbonate we essentially mean a mixture of carbonate and bicarbonate corresponding with a specific pH. The parasitic reactions of CO_2 with the alkaline electrolyte can cause a range of problems in CO_2 electrolyzers including (bi)carbonate precipitation and flooding of gas diffusion electrodes (GDEs), CO_2 crossover to the anode, low conversion and carbon utilization efficiency, electrolyte carbonation and pH-drift, negative impact on activity of the oxygen evolution reaction (OER) and CO2RR, decreased conductivity and increased cell voltages, and additional cost for CO_2 and electrolyte recycling, see Figure 1.[13−16] These issues are seriously hindering the scale-up and commercialization of low-temperature CO_2 electrolyzers.
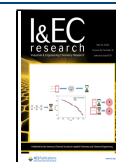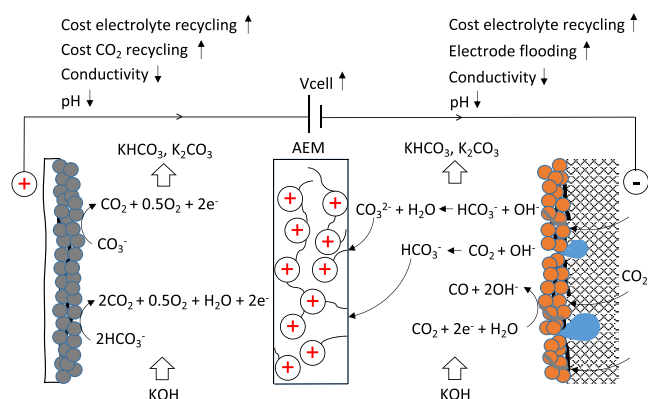
Figure 1. Illustration of the carbonation problem during CO_2 electrolysis. In the cathode compartment, (bi)carbonates are produced from the reaction of CO_2 and the generated hydroxides from CO_2 electrolysis. The (bi)carbonates are transported through the anion exchange membrane (AEM) and oxidized at the anode to release CO_2. The anolyte and catholyte are converted to (bi)-carbonates. The cell voltage (Vcell) increases due to a shift in the anode and cathode potentials due to a pH change.

For an alkaline flow cell, it has been estimated that up to 95% of CO_2 can be lost due to the parasitic carbonation effect, which essentially means that each CO_2 molecule has to be recycled 20 times for complete utilization.[17] The carbonation and crossover of CO_2 put a limit on the carbon efficiency of alkaline electrolyzers. For CO2R to CO in anion transporting cells, the maximum carbon efficiency is 50%,[18] while for ethylene this is 25%.[13,17] This has detrimental effects on the economics of any CO2R process that is performed in alkaline conditions.[19−21]

In this review, we provide (1) a reinterpretation of published results on CO_2 crossover in low-temperature CO_2 electrolyzers, (2) an overview of potential solutions to overcome or prevent the problems caused by electrolyte carbonation, (3) an estimation of the cost of recycling/recovering spent CO_2 and electrolytes, and (4) an outlook for future research to overcome carbon crossover in low-temperature CO_2 electrolysis. This review is not meant to be exhaustive and focuses primarily on carbon crossover and its consequences with a brief discussion on the related phenomena of GDE flooding. We aim to provide (1) a better understanding of the carbonation phenomena during CO2R, (2) a critical assessment of the proposed solutions and related costs, and (3) guidance regarding research priorities to solve one of the most pressing problems in the field of low-temperature CO_2 electrolysis.

2. CARBON CROSSOVER MECHANISM

As an example, we consider CO_2 electrolysis to CO in alkaline media. The half-cell reaction at the cathode for CO2R to CO can be written as

$$CO_2 + H_2O + 2e^- \rightarrow CO + 2OH^- \tag{R1}$$
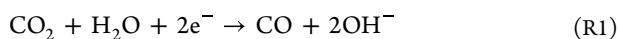
In aqueous (alkaline) media, the competing HER can also take place at the cathode according to the following reaction.

$$2H_2O + 2e^- \rightarrow H_2 + 2OH^- \tag{R2}$$
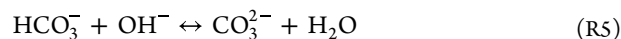
In acidic media, the HER is typically written as

$$2H^+ + 2e^- \rightarrow H_2 \tag{R3}$$

The produced hydroxides from the CO2R and the HER can react with freshly supplied CO_2 to form bicarbonate.
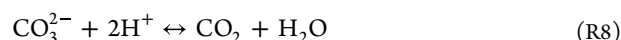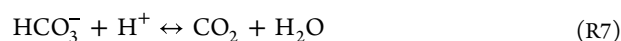
$$CO_2 + OH^- \leftrightarrow HCO_3^- \tag{R4}$$

In a subsequent step, the bicarbonate can react with an hydroxide ion to produce carbonate.

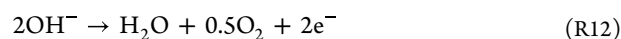$$HCO_3^- + OH^- \leftrightarrow CO_3^{2-} + H_2O \tag{R5}$$

The accompanying OER at the anode in acidic media can be written as

$$H_2O \rightarrow 2H^+ + 0.5O_2 + 2e^- \tag{R6}$$
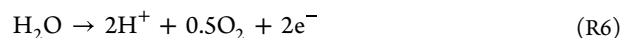
Using an anion exchange membrane (AEM) in the CO_2 electrolyzer, the bicarbonate, carbonate, and hydroxide ions from the cathode compartment will be transported to the anode compartment and neutralized with the protons from the OER (assuming acidic conditions) according to

$$HCO_3^- + H^+ \leftrightarrow CO_2 + H_2O \tag{R7}$$

$$CO_3^{2-} + 2H^+ \leftrightarrow CO_2 + H_2O \tag{R8}$$

$$OH^- + H^+ \leftrightarrow H_2O \tag{R9}$$

Combining the CO2RR with these neutralization reactions and neglecting the HER, it is possible to calculate the anodic gas composition ratio of CO_2 to O_2 if the only charge-carrier is HCO_3^-, CO_3^{2-}, and OH^- from the following reactions.

$$2HCO_3^- \rightarrow 2CO_2 + H_2O + 0.5O_2 + 2e^- \tag{R10}$$

$$CO_3^{2-} \rightarrow CO_2 + 0.5O_2 + 2e^- \tag{R11}$$

$$2OH^- \rightarrow H_2O + 0.5O_2 + 2e^- \tag{R12}$$
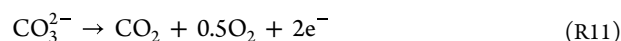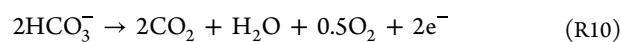
It is clear from reactions R10 to (R12) that the theoretical anodic gas composition ratio of CO_2 to O_2 will be 4, 2, and 0 if the transported ions through the AEM are HCO_3^-, CO_3^{2-}, and OH^-, respectively. Before moving to the experimental observations for the carbon crossover and the CO_2 to O_2 ratio, we will discuss the debatable assumption made by most of the previous studies that water is oxidized at the anode (i.e., reaction R6), while the conditions are (slightly) alkaline. It is more appropriate to write the OER in alkaline form to correctly represent the pH conditions.

$$2OH^- \rightarrow H_2O + 0.5O_2 + 2e^- \tag{R13}$$
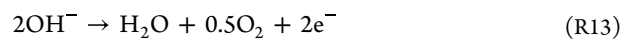
Clearly, the so-desired protons for the neutralization reactions, reactions R7 to (R9), are eliminated if hydroxides instead of water molecules are involved in the OER. As shown by Kötz et al.,[22] the reaction mechanism for OER involves hydroxides for pH > 4 and water for pH < 4. This is in agreement with the observations of Naito et al.[23] Typically, alkaline anolytes (e.g., KOH and $KHCO_3$ solutions) are used in AEM-based CO_2 electrolyzers. Therefore, the pH is near neutral to alkaline, and the OER should be written in hydroxide form. The consequence of this is that, instead of (bi)carbonate neutralization, a different mechanism is responsible for CO_2 evolution at the anode. A more likely mechanism, which does not require the cumbersome assumption of low pH at the anode, is the direct electro-oxidation of bicarbonate and carbonate to CO_2 according to reactions R10 and (R11), since bicarbonate and carbonate are thermodynamically easier to oxidize than water.[24] Now, the experimental observations of carbon crossover in alkaline CO_2 electrolyzers will be

discussed. The initial experimental studies on CO_2 crossover by Liu et al.,[25] Kaczur et al.,[26] and Larrazábal et al.[27] found an anodic CO_2 to O_2 ratio of 2:1, which essentially means that carbonate ions are the main charge-carriers across the AEM. Later, this observation has been confirmed by several studies but only at high current density CO2R.[28−32] Recent studies show that bicarbonate instead of carbonate is the main charge carrier in AEM-based CO2R at low current densities (roughly <100 mA/cm^2 for CO2R to CO).[33,34] For bicarbonate as the only charge-carrier, the CO_2/O_2 ratio at the anode is 4:1. Apparently, the mechanism for (bi)carbonate formation and crossover changes as a function of current density. In addition, we will see that the time-dependent response of the electrolysis system in terms of pH/conductivity changes, carbon species distribution, and carbon crossover is significantly influenced by the type, amount/flow and concentration of the electrolytes (anolyte and/or catholyte), the CO_2 supply rate, and cell configuration (zero-gap MEA, flow cells, etc.). We will discuss these effects at high and low current densities separately in Section 2.1 and Section 2.2, respectively.

2.1. Carbon Crossover at High Current Density. Ma et al.[28] presented a detailed study on (bi)carbonate crossover during CO2R to hydrocarbons using a GDE-based flow cell and a Cu catalyst. An anion exchange membrane with different anolytes and catholytes (1 M KHCO$_3$, 1 M KOH, and 5 M KOH) was used. For 1 M KHCO$_3$ as anolyte and catholyte, these authors observed at a CD of 200 mA/cm^2 that the anodic gas composition ratio of CO_2/O_2 gradually decreased from roughly 3 to 2, which implies that the main charge-carrier changed from a mixture of HCO_3^-/CO_3^{2-} to pure CO_3^{2-} during the course of the experiments. The pH of the catholyte was changed from the initial value of 8.3 to ~11.5 after an electrolysis time of 7 h due to the conversion of bicarbonate to carbonate. The pH of 8.3 and ~11.5 corresponds to the pH of 1 M KHCO$_3$ and 0.5 M K$_2$CO$_3$ solutions, respectively. The pH of the anolyte was rapidly reduced from 8.3 to 7.9 but remained at this value for the rest of the electrolysis experiment. The final pH of 7.9 corresponds to the pH of 1 M KHCO$_3$ solution saturated with CO_2. Ma et al.[28] observed an anodic CO_2/O_2 ratio of 2 for other current densities as well (150, 250, and 300 mA/cm^2), which means that the main charge carrier is the carbonate ion for CDs $\geq$ 150 mA/cm^2. However, the transition rate of the catholyte from bicarbonate to carbonate was accelerated at higher CDs. For 1 M KOH as anolyte and catholyte, no CO_2 was detected at the anode for the first 2.5 h of electrolysis. CO_2 started to evolve after this equilibration period, and the anodic gas composition quickly reached a CO_2/O_2 ratio of 2. The pH of the anolyte and catholyte reduced after 5 h of electrolysis time from 13.6 to 11.6 and 8, respectively. It is clear that the catholyte was converted from OH$^-$ to CO_3^{2-}, which crosses over through the AEM and oxidizes at the anode. Ma et al.[28] put forward that 'the anolyte was neutralized by H$^+$ produced in the anodic reaction R6, thus slowly decreasing the anolyte pH'. As explained earlier, this is a debatable explanation, because OER should be written in alkaline form (reaction R13), since the conditions in the anode compartment are alkaline. We will provide an alternative explanation for the observed phenomena at the anode without relying on the questionable assumption of low local pH in an alkaline solution. It is more plausible that the carbonate ions cross over through the AEM and are directly oxidized at the anode, because (bi)carbonates are thermodynamically easier to oxidize than water. The produced

CO_2 at the anode is then absorbed/bubbled into the KOH solution, which gradually converts into a K$_2$CO$_3$ solution. After 2.5 h, almost all KOH is consumed, and the formed HCO_3^-/CO_3^{2-} buffer will start to release CO_2 into the gas phase if the pH drops below 9, because CO_2 can only exist under these conditions. However, even at a higher pH, CO_2 can be released into the gas phase if the system operates under nonsteady conditions where the CO_2 bubbling rate is much higher than the CO_2 absorption rate. Haspel and Gascon[32] observed CO_2 release into the anodic gas phase at a pH higher than 10, which can only be explained by this unsteady behavior. The initial absorption rate of CO_2 in KOH solutions is almost a factor 10 higher than that of K$_2$CO$_3$ solutions. This means that the absorption rate of CO_2 in KOH solutions is high enough to keep up with the bubbling rate of CO_2 even at very high CDs, but this might not be the case for K$_2$CO$_3$ solutions. Note that, if the anolyte is recirculated, CO_2 bubbling will convert the K$_2$CO$_3$ solution into KHCO$_3$ according to

$$CO_3^{2-} + H_2CO_3 \leftrightarrow 2HCO_3^- \tag{R14}$$
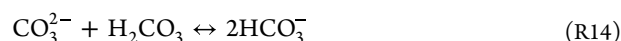
This is consistent with the observation of Ma et al.[28] that the anolyte pH was ~8 after 5 h of electrolysis time (i.e., the pH of 1 M KHCO$_3$ saturated with CO_2 is roughly 8). In a second study, Ma et al.[31] investigated the effect of different membranes (AEM, cation exchange membrane (CEM), and bipolar membrane (BPM)) on the crossover phenomena. At a CD of 200 mA/cm^2 and with 1 M KHCO$_3$ as anolyte and catholyte, the AEM-based cell showed a similar behavior as discussed earlier (CO_2/O_2 ratio of 2). For the CEM-based cell, a CO_2/O_2 ratio of 4 was observed at the anode, and the pH of the catholyte (anolyte) was increased (decreased) from 8.3 to 9.8 (8.3 to 6.7) during 3 h of electrolysis time. The experiments were stopped after 3 h, because the conductivity of the anolyte decreased from 70 to 3 mS/cm due to the depletion of cations. A CO_2/O_2 ratio of 4 can be explained by the fact that bicarbonate from the electrolyte is oxidized at the anode as soon as the K$^+$ ion is transported through the CEM. This essentially means that the bicarbonate from the anolyte is consumed, while the potassium ions are accumulated in the catholyte. For the BPM-based cell, the anodic CO_2/O_2 ratio decreased from 1 to 0.3 in the first 4 h and stabilized around 0.25 after 10 h. The pH of the anolyte increased slightly from 8.3 to 9.6, while the pH of the catholyte remained nearly constant after 10 h. The initial 1 M KHCO$_3$ anolyte reacts with the OH$^-$ from the BPM and is converted to 0.5 M K$_2$CO$_3$, which is consistent with the observed conductivity of ~68 mS/ cm. Since the BPM does not allow (bi)carbonate crossover, the small amounts of CO_2 at the anode should come from a different source. We hypothesize that the source is either due to the crossover of dissolved CO_2, which is uncharged and thus not repelled by the ion exchange layers of the BPM, or the BPM is simply not 100% selective and allows some (bi)carbonates to cross over. Furthermore, the (bi)carbonates generated at the cathode are neutralized with the protons from the BPM and cause CO_2 release in the cathode compartment. We note that the bicarbonate from the electrolyte (KHCO$_3$) is not converted to CO_2 due to charge neutrality constraints. Haspel and Gascon[32] studied (bi)carbonate crossover in a hybrid flow/membrane electrode assembly (MEA) cell (i.e., with alkaline anolyte, but no liquid catholyte) using KOH and KHCO$_3$ anolytes at different current densities. These authors recorded the pH and conductivity of the anolyte, the cell voltage, and the evolved gas at the anode and cathode for

different current densities as a function of time. Haspel and Gascon[32] also observed an anodic CO_2/O_2 ratio of ~2 for CO2R at high CDs (≥100 mA/cm^2). At low CDs, the anodic CO_2/O_2 ratio was between 2 and 4, which means that the main charge carrier changed consecutively from carbonate to a mixture of carbonate and bicarbonate to purely bicarbonate as the CD decreased from ≥100 to 2.5 mA/cm^2. The pH of the initial 1 M KOH anolyte decreased from 14 to 7.7, which corresponds to a pH of 1 M KHCO$_3$ solution that is saturated with CO$_2$. Accordingly, the conductivity of the anolyte decreased from ~220 mS/cm (1 M KOH) to 80 mS/cm (1 M KHCO$_3$). Clearly, the initial 1 M KOH anolyte is converted to KHCO$_3$ at the end of the experiment. For 1 M KOH as anolyte, Haspel and Gascon[32] did also not observe any CO$_2$ in the gas phase for the first 2 h of experiments, which is consistent with the findings of Ma et al.[28] In this time frame, CO$_2$ from the oxidation of (bi)carbonate is absorbed by the KOH solution, which is first converted to K$_2$CO$_3$. Finally, the K$_2$CO$_3$ solution is converted to KHCO$_3$ upon continuous bubbling of CO$_2$. The conversion rate of KOH to KHCO$_3$ was faster for higher CDs. As can be seen in the Supporting Information of Haspel and Gascon,[32] CO$_2$ in the anodic gas mixture was only observed when the pH of the anolyte was below 9 for experiments at low current densities (≤100 mA/cm^2). At high CDs (>100 mA/cm^2), CO$_2$ in the anodic mixture was also observed at higher pHs, which is due to the unsteady behavior discussed before. In this case, the CO$_2$ absorption rate in the (bi)carbonate solution is lower than the CO$_2$ evolution rate causing CO$_2$ release into the gas phase. The experiments of Haspel and Gascon[32] support our hypothesis that (bi)carbonates are directly oxidized at the anode to CO$_2$, which bubbles into the alkaline solution and converts KOH to KHCO$_3$ in the long run. CO$_2$ is released into the gas phase when the pH drops below 9 or when the absorption rate of the solution is lower than the CO$_2$ generation rate, which is typically the case at high CD electrolysis. Our explanation of the CO$_2$ evolution phenomena at the anode is also supported by the bubbling experiments of Zhong et al.[35] These authors recorded the pH change of different electrolytes (K$_2$CO$_3$, KHCO$_3$, KOH, KCl, and HCl) upon bubbling with CO$_2$ and noticed a very similar time-dependent behavior of the pH as reported by Ma et al.[28] and Haspel and Gascon.[32]

Haspel and Gascon[32] performed an interesting experiment in an attempt to better understand CO$_2$ hydration and carbon crossover during HER under CO$_2$-rich conditions. Like CO2R to CO, the HER, reaction R2, also produces two hydroxide ions, which can and ideally should react to (bi)carbonate under CO$_2$-rich conditions. These authors used commercially available GDE-type cathodes (Pt/C, IrO$_2$, and NiFeCo/Ni paper) that have a high activity for the HER but a low activity for CO2R to decouple HER from CO2RR. In the experiment, the CD was 150 mA/cm^2, 1 M KHCO$_3$ was used as catholyte, and 60 mL/min of CO$_2$ was supplied to the cathode. One would expect a similar carbon crossover mechanism if the local environment for (bi)carbonate formation is identical for HER and CO2R. Surprisingly, the carbon crossover for HER in a CO$_2$-rich environment was lower than under CO2RR conditions. Under HER, the CO_2/O_2 ratios for Pt/C, IrO$_2$, and NiFeCo/Ni were 1.1, 0.8, and 0.7, respectively. These ratios are two times lower than the expected theoretical CO_2/O_2 ratio of 2 for carbon crossover due to carbonate transport in AEM-based CO$_2$ electrolysis. On the other hand, using a

catalyst that is active for CO2R (Ag/C), Haspel and Gascon[32] observed a CO_2/O_2 ratio of 2 under similar conditions as the HER under CO$_2$-rich environment. From these experimental findings, Haspel and Gascon[32] concluded that 'hydroxide is not just hydroxide' and CO$_2$ hydration is unidentical under HER and CO2R conditions. Recently, Moss et al.[36] used an MEA-based setup with an AEM to study CO$_2$ reduction on a Cu catalyst. No catholyte was used in the experiments, while KHCO$_3$ was used as anolyte. These authors observed a CO_2/O_2 ratio of roughly 2 at the anode for CO$_2$ electrolysis at 100 and 150 mA/cm^2. At 200 mA/cm^2, the CO_2/O_2 ratio at the anode fluctuated between 2 and 1, while at 250 mA/cm^2 the CO_2/O_2 ratio was roughly 1. Using operando XRD, Moss et al.[36] observed (bi)carbonate formation in the GDE, which causes an increase in the HER. This increase in HER results in a drop in the cell potential due to a shift in the ion transport mechanism through the AEM from carbonates to hydroxides. During CO$_2$ electrolysis at 250 mA/cm^2, the HER dominated, and a CO_2/O_2 ratio of 1 was observed at the anode. This observation of Moss et al.[36] is similar to the observation of Haspel and Gascon[32] that the CO_2/O_2 ratio at the anode for HER under a CO$_2$-rich environment is roughly 1. It is currently unclear why CO$_2$ hydration is unidentical under HER and CO2R conditions.

2.2. Carbon Crossover at Low Current Density. In the previous section, we have seen that high-CD CO2R results in carbonate crossover through the AEM to the anode. At low CDs, the main charge carrier is the bicarbonate ion. Lin et al.[33] studied (bi)carbonate crossover in a flow cell with 1 M KHCO$_3$ as the anolyte and catholyte. CO2R was performed at 10, 30, and 50 mA/cm^2 using an AEM, CEM, and BPM. For the AEM-based system, it was shown for all CDs that bicarbonate was the main charge carrier causing CO$_2$ crossover and limiting the utilization efficiency to 14.4%. The CEM-based system exhibited low utilization efficiencies due to recirculation between the anolyte and the catholyte to prevent depletion of cations from the anolyte. The BPM-based CO$_2$ cell showed significantly higher utilization efficiencies (up to 61.4%) compared to the AEM-based electrolyzer. Eriksson et al.[34] presented a detailed study on CO$_2$ crossover in AEM and BPM-based CO$_2$ electrolyzers. These authors performed CO2R at 45 mA/cm^2 using a GDE-based flow cell with 1 M KHCO$_3$ and 1 M KOH as catholyte and anolyte, respectively. No CO$_2$ was detected in the anodic gas mixture for the first 12 h of electrolysis, which is due to the absorption of CO$_2$ by the KOH solution. After 12 h, CO$_2$ started to evolve in the gas phase and the CO_2/O_2 ratio in the anodic mixture quickly stabilized at 3.8, suggesting the bicarbonate was the main charge carrier. The pH of the initial 1 M KOH anolyte changed from 14 to 8 following a typical CO$_2$ bubbling curve as also observed by Zhong et al.,[35] Ma et al.,[28] and Haspel and Gascon.[32] The KOH solution is first converted to K$_2$CO$_3$ and then to 1 M KHCO$_3$, which has a pH close to 8 when saturated with CO$_2$. The catholyte pH remained constant at a value of ~8 during the course of the experiment. This is different from the high CD experiments of Ma et al.[28] where the pH of the catholyte was increased from 8 to 11.6 due to the conversion of bicarbonate to carbonate. The reason for this is the low generation rate of hydroxide ions for low-CD conditions and the high supply rate of CO$_2$ to the cathode. As a consequence, bicarbonate is formed according to reaction R4, but reaction R5 cannot proceed due to the lack of hydroxide ions, which are consumed by the excess supply of

CO_2. For the BPM-based experiments with 1 M KOH as anolyte and 1 M $KHCO_3$ as catholyte, Eriksson et al.[34] did not observe any CO_2 in the anodic gas mixture during CO2R at 45 mA/cm^2 for 16 h. The pH of the anolyte was only decreased slightly from the initial value of 14 to 13.6 at the end of the experiment. When the anolyte was changed from 1 M KOH to 0.1 M KOH, CO_2 evolved in the gas phase and the observed anodic CO_2/O_2 ratio was 0.4, which is almost a factor 10 lower than the AEM-based cell. Clearly, the crossover of CO_2 from the cathode to the anode is significantly reduced but not completely prevented with a BPM-based cell. Likely dissolved CO_2, which is not charged and thus not retained by the ion exchange layers in the BPM, crosses over from the cathode to the anode and slowly adds carbonate to the electrolyte. The exact mechanism of CO_2 crossover in BPM-based cells is still unclear and should be corroborated by future studies.

Lu et al.[37] provide an excellent understanding of the carbonation phenomena near the electrode surface. These authors used in situ Raman spectroscopy to probe the local pH near a CO2R GDE under working conditions (50 and 100 mA/cm^2) for different catholytes (1 M KOH and 1 M $KHCO_3$). Under open-circuit conditions (i.e., 0 mA/cm^2), 1 M KOH catholyte flow at 0.5 mL/min, and a CO_2 flow of 20 sccm, the local pH was ~7 at the cathode surface and increased to ~11 over a distance of 120 μm away from the electrode into the electrolyte solution. Under these conditions, the supplied CO_2 reacts with KOH at the electrode/electrolyte interface to form bicarbonate, which is converted to carbonate upon diffusion into the electrolyte solution. Accordingly, the concentration of bicarbonate decreased from 0.22 to 0.024 M, while the concentration of carbonate increased from 0.065 to 0.20 M for measurements at 10 and 120 μm away from the electrode surface, respectively. For increasing CO_2 supply rates (5 to 25 sccm), it was shown that more CO_2 reacts with the alkaline solution and the pH gradient region becomes wider. Lu et al.[37] then performed CO2R to CO in a GDE-based flow cell and used in situ Raman measurements to probe the local pH near the electrode surface. At 50 mA/cm^2 and 1 M KOH as catholyte, the concentration of bicarbonate (carbonate) decreased (increased) from 0.23 to 0.029 M (0.07 to 0.14 M) for measurements at 10 and 80 μm away from the electrode surface, respectively. Clearly, the generated bicarbonates at the electrode/electrolyte interface diffuse into the electrolyte and are converted to carbonates (see Figure 2), but the bicarbonate region is 40 μm narrower compared to the open-circuit case. The local pH at the electrolyte/electrode interface at 50 mA/cm^2 was ~9, which is higher than the open-circuit case (pH of ~7). At 100 mA/cm^2, the bicarbonate region is reduced further and the local pH at the electrode surface increased to 9.8. At 150 mA/cm^2, only carbonate and no bicarbonate was observed near (10 μm away) the electrode surface, which suggests that the local pH was >12. These experiments provide a clear picture of the carbonation phenomena near the electrode surface. For 1 M KOH catholyte, CO_2 reacts with the hydroxides from the CO2RR and the electrolyte to first produce bicarbonate, which is then converted to carbonate regardless of the CD, but the conversion rate is increased at higher CDs. Hence, the conversion of bicarbonate to carbonate depends on the availability of hydroxide ions. At sufficiently high CDs, the conversion rate of bicarbonate to carbonate is so high that only carbonate is observed near the electrode. As shown by Lu et al.,[37] the response of the system is different if 1 M $KHCO_3$ (instead of KOH) is used as the catholyte. For 1 M
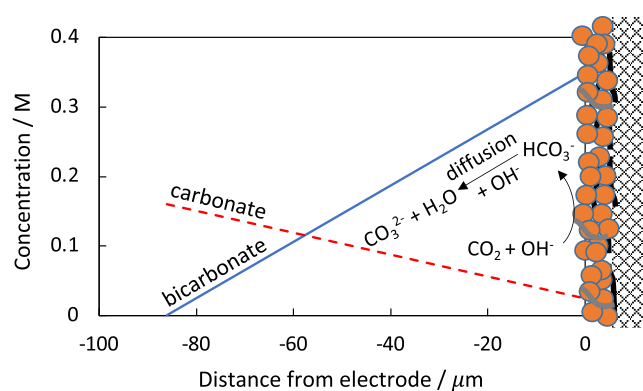

Figure 2. Concentration profiles of bicarbonate and carbonate near the electrode for CO_2 electrolysis at 50 mA/cm^2. One M KOH was used as catholyte. Data based on Lu et al.[37] show that bicarbonates are mostly generated near the electrode, which diffuse into the solution and are rapidly converted to carbonates due to the alkaline electrolyte.

$KHCO_3$ as catholyte and under open-circuit conditions with CO_2 supply to the cathode, no carbonate was observed near (up to 120 μm away) the electrode surface, while in the bulk (>120 μm) carbonate was detected in a ratio that corresponds with the pH of the solution. This is clear evidence that reaction R14 occurs when CO_2 is bubbled into a bicarbonate solution. At 50 mA/cm^2, the concentration of bicarbonate (carbonate) increased (decreased) from 0.11 to 1.26 M (0.61 to 0.18 M) for measurements at 10 and 130 μm away from the electrode surface, respectively. The bicarbonate of the electrolyte reacts with the OH$^-$ generated from the CO2RR to form carbonate, which diffuses into the catholyte and is converted back to bicarbonate due to the acid–base equilibria. The local pH at the cathode surface was 11.9, but the pH decreased to ~9.5 at a distance of 120 μm away from the electrode. Note that the concentration and pH profiles are completely opposite to what was observed for KOH as the catholyte.

Henckel et al.[38] used surface-enhanced Raman spectroscopy to study the local pH during CO2R on a Cu catalyst using an alkaline flow electrolyzer. These authors also observed a substantially lower local pH than expected from the bulk pH. The local pH was shown to depend on the applied potential, and the decreases in the pH were associated with the formation of malachite $[Cu_2(OH)_2CO_3]$. These results show that the local CO2R environment can differ significantly from the bulk and several unexpected phenomena can be observed near the electrode surface.

In summary, the time-dependent behavior of the carbonation phenomena is extremely complex and influenced by initial and operating factors such as the type and concentration of the electrolytes, the flow rate of CO_2 and the electrolytes, the actual amount of anolytes and catholytes, the temperature and pressure, and the cell configuration (e.g., type of membranes). All these parameters/factors should be considered and carefully set in experiments for a proper understanding of the carbonation effect and to allow a meaningful comparison between different studies. We feel that more experimental and theoretical work is required to elucidate the carbon crossover mechanism. This understanding is crucial for finding a cost-effective solution to the carbonation problem.

3. FLOODING OF GAS DIFFUSION ELECTRODES

The carbonation phenomena is closely linked to the flooding problem of gas diffusion electrodes during CO2R. Flooding is the penetration of electrolyte into the pores of the gas diffusion layer (GDL). This penetration of the electrolyte increases diffusion pathways and prevents the CO_2 to reach the active sites on the catalyst surface. Flooding affects the performance of the GDE in different ways as it increases the HER, because the aqueous electrolyte is directly exposed to the carbon in the GDL, and it causes salt precipitation, which leads to permanent blocking of the GDL pores.[39,40] The exact mechanism of GDE flooding has yet to be elucidated, but the factors that seem to play an important role are (1) leakage of electrolytes into the GDE due to electrowetting effects, (2) formation/precipitation of salt crystals on and inside the GDE due to electrolyte carbonation, (3) decreasing hydrophobicity of the GDE after high current application, (4) the pressure drop across the GDE that is determined by the cell configuration (flow-through or flow-by), (5) defects or cracks in GDEs, and (6) GDE degradation due to mechanical compression, erosion by gas flow, dissolution of electrode materials in the catholyte, delamination of the layers, and corrosion, see Figure 3.[41]
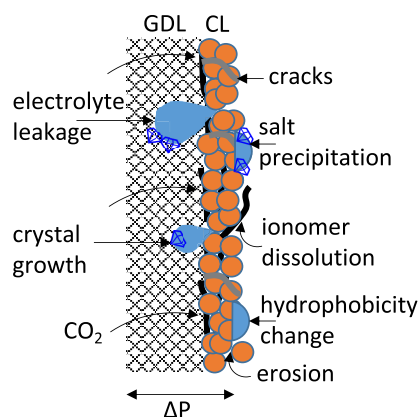

Figure 3. Different mechanisms that contribute to electrode flooding. GDL is gas diffusion layer, and CL is catalyst layer.

We will present a brief overview of the key findings of recent GDE flooding studies. The reader is referred to the excellent perspective of Sassenburg et al.[42] for more information on salt precipitation and GDE flooding in zero-gap CO_2 electrolyzers.

Leonard et al.[43] studied GDE flooding in an alkaline flow cell (flow-by mode) for CO_2 conversion to CO on a silver-based catalyst. These authors found that flooding was accelerated by current passage causing electrowetting and reduced GDE hydrophobicity, and carbonate formation/precipitation, which facilitated electrolyte permeation. In a follow-up study, Leonard et al.[44] studied the role of electrode wettability in CO_2 electrolyzers for liquid products. These authors used contact angle measurements, electrolyzer mass balances, and capillary pressure models to relate the concentrations of the liquid products to cell operating conditions and to estimate the pressure drop across the GDE that might result in electrode flooding. Using this model, Leonard et al.[44] estimated that GDEs that produce alcohol products with a concentration of <30 wt % are more susceptible to flooding, while formic acid electrolyzers are more resistant to electrode flooding. Yang et al.[39] investigated the role of carbon-based gas diffusion layers (GDLs) on GDE

flooding during CO2R. These authors found that the applied potential plays an important role in GDE flooding as it affects the wetting characteristics and hydrophobicity of the GDL. Cofell et al.[45] investigated the effect of electrolytes on carbonate formation and GDE flooding in an alkaline CO_2 electrolyzer (flow-through mode). The performance of the CO2R cell diminished due to degradation of the GDE as a consequence of carbonate deposits on the electrode surface. The type and concentration of the electrolyte had a large effect on the carbonate formation rate, morphology, distribution, and surface coverage of the deposits. Cofell et al.[45] showed that the cell performance reduced dramatically after ∼50% of the catalyst surface was occluded with the carbonate deposits, which reduced the hydrophobicity of the GDE and induced flooding of the electrode. Disch et al.[46] used high-resolution neutron imaging to study salt precipitation and water transport in a zero-gap CO_2 electrolyzer under industrially relevant conditions (200 mA/cm^2, cell voltage of 2.8 V, and CO FE of 99%). These authors observed salt precipitation and associated electrode flooding throughout the entire experiment. The precipitation and accumulation of salts was more severe at higher CDs, which heavily influenced the water distribution in the cathode and caused local dry-out and hotspots. Furthermore, a higher salt accumulation was visible under the cathode channel of the flow field than in other regions. These results support the hypothesis that precipitated salts penetrate the gas diffusion layer and block the transport of CO_2 to the catalyst layer, which initiates the HER and reduces the FE of CO2R. Kong et al.[47,48] used energy-dispersive X-ray (EDX) mapping and inductively coupled plasma mass spectrometry (ICP-MS) to study GDE flooding in a zero-gap CO_2 electrolyzer. The EDX/ICP-MS tool was used to quantify the flooding phenomena by measuring the potassium concentration as a function of the GDE depth. These authors studied different types of GDLs and found that GDEs that bear cracks in the microporous layer are less susceptible to flooding. Kong et al.[47,48] hypothesized that the fibrous layer of the GDE, which is water/electrolyte accessible through the cracks, serves as a reservoir for flooding and can prevent flooding-associated degradation of the catalyst layer. However, it is very likely that the flooding is only postponed and will affect once the macroporous layer is fully saturated.

4. POTENTIAL SOLUTIONS FOR SALT FORMATION

From the foregoing discussion, it is clear that electrolyte leakage into the GDE and subsequent precipitation and crystallization of salts in the pores of the GDL play an important role in the performance degradation of GDE-based CO_2 electrolyzers. Different (partly successful) strategies have been presented in the literature to overcome/diminish the disastrous flooding effect. Sassenburg et al.[42] identified four main categories of engineering solutions to prevent salt precipitation. These approaches include (1) passively modifying the type and concentration of the anolyte, (2) actively dissolving precipitates in the GDE, (2) actively pulsing the reactor, and (4) passively modifying the MEA.

It is important to note that salts can only be formed if a cation is combined with an anion. Hence, the first category of solutions aims to reduce or completely eliminate cations from the anolyte and/or catholyte. Using dilute anolyte (10 mM $KHCO_3$), Liu et al.[25] demonstrated stable CO2R to CO for 3800 h of operation at 200 mA/cm^2. As shown by Cofell et al.,[45] the type of cation can also have significant influence on

the precipitation/crystallization behavior of the formed (bi)carbonates. Therefore, the type and concentration of the electrolyte can influence the flooding effect. The drawback of using dilute or no electrolytes is the increased cell resistance/overpotential and missing the potential benefits of cations in CO_2 reduction (e.g., stabilization of key intermediates).[49] The second category of solutions aims to (periodically) inject solvents (deionized water or electrolytes) into the GDE to dissolve accumulated salts from the pores and to provide cations near the electrode surface (cathode activation). Examples of this category have been reported by Endrödi et al.[50] and De Mot et al.[51] The drawback of this solvent injection approach is that the performance is only temporarily recovered, the HER is initiated if water droplets are retained in the pores after rinsing, and a high differential pressure is required to penetrate the pores of the hydrophobic GDE, while commonly used GDEs have a narrow pressure stability window (~100 mbar). The third category of solutions prevents salt accumulation by periodically switching between an operational voltage and a regeneration voltage. At a higher operational voltage/CD salts are accumulated, while (bi)carbonates are removed during the lower regeneration voltage/CD due to electromigration. Xu et al.[52] used this potential switching approach (3.8 V during operation and 2.0 V during regeneration) to demonstrate stable cell operation for 157 h (total 236 h including regeneration) without salt formation and performance degradation. The main drawback of this approach is the downtime (33% in the case of the experiments of Xu et al.),[52] which will significantly affect the productivity and capital cost of the process. The last category of solutions uses membranes, GDE materials, and reactor configurations that can inhibit/prevent salt formation. Wu et al.[53] studied the effects of the microporous layer (MPL) on the flooding of GDEs and found that a thick MPL minimized flooding. In a follow-up study, Wu et al.[53] used a vacuum-assisted infiltration method to embed submicron polytetrafluoroethylene (PTFE) particles at the interface of the MPL and the GDL. This PTFE-embedded GDL significantly reduced electrolyte seepage and maintained a CO_2 to CO FE of >80% at 100 mA/cm^2 for more than 100 h. Baumgartner et al.[54] investigated GDE flooding during CO2R to CO using woven (carbon cloth) and nonwoven (carbon paper) GDLs. These authors showed that carbon-paper-based GDEs suffered from electrowetting and CO FE loss at high CDs (>200 mA/cm^2). Conversely, the carbon-cloth-based GDE sustained a CO FE of >55% at 180 to 200 mA/cm^2 and 10 V for over 125 h despite a high differential pressure of 100 mbar, which caused flooding and continuous liquid breakthrough. This performance was attributed to the bimodal pore size distribution (PSD) of the carbon cloth, where the electrolyte is preferentially drained through the larger pores, while the smaller pores are available for gas transport. McCallum et al.[55] used a numerical model to screen reaction conditions and membrane properties to reduce crossover of carbonate and liquid products during CO2R. Based on this multiphysics model, these authors state that a decreasing CO_2 partial pressure and increasing CD, while keeping the concentration of CO_2 sufficient at the catalyst surface, will substantially mitigate carbon formation and that CO_2 utilization can be increased with thin membranes. This conclusion essentially means that the concentration of CO_2 should be at a level that supports efficient CO2R, but low enough to prevent the carbonation reaction R4. It remains

unclear how in practice a high CO2R CD can be achieved with a dilute CO_2 stream.

In the previous section, we have discussed engineering solutions that mainly reduced salt formation but did not eliminate CO_2 crossover. In the following sections, we will discuss potential solutions for both carbon formation and CO_2 crossover. These solutions (use of bipolar membranes, electrolysis in acidic media, cascade electrolysis, and electrolysis of reactive solutions) can possibly be placed in category four of Sassenburg et al.[42]

5. POTENTIAL SOLUTIONS FOR CARBON CROSSOVER

The carbonation phenomena has a detrimental effect on the CO_2 utilization and the economics of CO_2 electrolyzers. The scale-up and commercialization of low-temperature CO_2 electrolyzers require a cost-effective solution to the carbonation problem. In the following, we will provide a summary and a critical assessment of the solutions proposed in the literature.

5.1. Electrolysis in Acidic Media. In principle, the most straightforward solution to the carbonation phenomena is CO2R in acidic media, because the main cause of the problem is related to the hydroxides generated at the cathode. That is easier said than done. In the past, CO2R in acidic media has been discouraged due to excessive hydrogen evolution at the cathode. However, recent studies show promising results for CO2R in (slightly) acidic media. We note that there is clear evidence that water, instead of H$^+$, is involved in the CO2R mechanism, as ascertained by Bondue et al.[56] and Hori.[57] As a consequence, hydroxides will always be generated at the cathode, but these hydroxides or the formed (bi)carbonates will be neutralized immediately in an acidic environment.

The first successful attempt for CO2R in highly acidic media (pH < 1) was reported by Huang et al.[58] These authors obtained a relatively high FE (~50%) toward multicarbon products at a high CD (1.2 A/cm^2), a single-pass conversion of ~77%, and a cell voltage of 4.2 V by concentrating potassium cations near the electrode surface using a cation-augmenting strategy to accelerate CO_2 activation and enable efficient CO_2 electrolysis in highly acidic media (pH < 1). The work of Huang et al.[58] is considered groundbreaking for several reasons, as it demonstrates (1) relatively efficient CO2R in highly acidic conditions, something that was thought impossible thus far, (2) that carbon−carbon (C−C) coupling, a process that is favorable in alkaline conditions, can be promoted in acidic media, and (3) that carbon crossover can be eliminated if CO2R is performed in highly acidic media (only oxygen evolution was observed at the anode). Recently, Xie et al.[59] used density functional theory studies to design a Pd−Cu-based catalyst to selectively convert CO_2 to C$_{2+}$ products in highly acidic media (pH of 2). These authors obtained an FE of ~90% for CO_2 to C$_{2+}$ at 500 mA/cm^2 with a single-pass CO_2 conversion of 60% to C$_{2+}$ and with negligible product and carbon crossover. The high efficiency and activity of the Pd−Cu catalyst for CO2R in acidic media was attributed to its ability to strongly bind CO* (the key intermediate for C−C coupling) and suppress H* (the key intermediate for HER) adsorption through adsorbate−adsorbate interactions. Despite these promising results, CO2R in acidic media needs to be optimized for better selectivities, lower cell voltages, and efficient oxidation reactions in acidic media at the anode using non-noble metals.

The promoting effect of cations on CO2R was recently also observed by Endrödi et al.[50] in a water-fed zero-gap CO_2 electrolyzer. These authors used an in situ cathode activation strategy by periodically injecting alkali cation-containing solutions into the GDE. This enabled high rate CO2R in deionized water-fed electrolyzers (pure water was transported from the anode to the cathode through an AEM) with limited performance decrease over a time period of >200 h. No physical (bi)carbonate precipitation was observed in the cell, but the CO_2/O_2 ratio at the anode was 2:1. Clearly, the (bi)carbonate crossover problem was not solved by this alkali activation strategy, but the precipitation of (bi)carbonates and the related flooding of the GDE were circumvented.

Pan et al.[60] used an acid-fed CEM-based MEA to demonstrate CO2R to CO with a partial CD of up to 105 mA/cm^2 at 4 V with an optimal FE and single-pass conversion of ~80% and ~90%, respectively. These authors used an acidic anolyte (H_2SO_4 + M_2SO_4 mixtures with M = H^+, Li^+, Na^+, K^+, and Cs^+) and supplied humidified CO_2 to the cathode to eliminate (bi)carbonate crossover. The cation had a strong effect on the FE of CO, which was roughly increased from 8% to 77% in the order of H^+ < Li^+ < Na^+ ≈ K^+ < Cs^+. More importantly, Pan et al.[60] showed that (bi)carbonate precipitation occurred at the cathode for relatively high concentrations of cations (0.01 M H_2SO_4 + x M M_2SO_4, where x ≥ 0.1). The cations cross over from the anode to the cathode and participate in the carbonation reaction. These authors mentioned that a relatively low CD and dilute electrolytes with an H^+ to Cs^+ ratio of 1:1 (e.g., 0.01 M H_2SO_4 + 0.01 M Cs_2SO_4) are the optimal conditions to obtain high FEs for CO and eliminate (bi)carbonate formation/precipitation. The optimal conditions are determined by a delicate balance between the (bi)carbonation formation rate and the proton flux from the anode. For a very low H^+ to Cs^+ ratio, the H^+ flux to the cathode is insufficient to neutralize the (bi)carbonates, which cause precipitation and performance loss. Conversely, for a high H^+ to Cs^+ ratio, the flux of protons is too high, which initiates the HER. The main problem with the cell configuration used by Pan et al.[60] is that, after some time, the cations (i.e., the Cs^+) in the anolyte will be depleted and promote the HER due to an increased H^+ to Cs^+ ratio. However, the work of Pan et al.[60] is in agreement with the observations of Monteiro et al.[61] and Singh et al.[62] that the cation acidity, hydration, and hydrolysis play an important role between hydrogen evolution and CO2R. The accumulation of alkali cations near the electrode surface at the outer Helmholtz plane (OHP) influence the HER and the CO2RR in different ways; (1) it inhibits the access of protons to the catalyst surface and, thus, suppresses the HER, (2) the hydrated cations increase the interfacial electric field, which is beneficial for the adsorption of CO2R intermediates (e.g., *CO_2 and *CO), and (3) cation hydrolysis near the cathode leads to higher local CO_2 concentrations due to a buffering effect, which increase the activity and selectivity of CO2R. Singh et al.[62] demonstrated that the cation hydration number and the pK_a for cation hydrolysis decrease with increasing cation size. The pK_a of K^+, Rb^+, and Cs^+ ions was shown to be sufficiently low to act as a buffering agent. Monteiro et al.[63] showed that the CO2RR on Cu, Au, and Ag electrodes did not occur when no metal cations were added to the solution. These authors provide clear evidence that cations play a crucial role in stabilizing the key reaction intermediates.

The recent works of the Koper group greatly contribute to our understanding of the HER and the CO2RR in (slightly) acidic media.[56,61,63−69] As demonstrated by Bondue et al.,[56] CO2R in acidic electrolytes does not necessarily result in excessive hydrogen evolution. These authors showed that hydrogen evolution and (bi)carbonate formation are determined by a delicate balance between CO2R, water reduction, and proton reduction in acidic media. Hydrogen evolution can almost completely be eliminated if the proton flux toward the cathode is balanced with the hydroxide flux generated from the CO2RR. In this case, the protons are neutralized by the hydroxides (reaction R9) before they reach the cathode and participate in the HER. A deficit in protons will result in (bi)carbonate formation according to reaction R4, while an excess of protons will cause hydrogen evolution according to reaction R3. These results imply that efficient CO_2 electrolysis and elimination of (bi)carbonate formation are possible in acidic media if the rate of CO2R (i.e., OH^- generation) can be matched with the mass transfer rate of protons to the electrode surface. We can qualitatively explain these design principles by invoking the schematic triangular diagram from our previous work,[70] see Figure 4. Note that, being a qualitative diagram, the
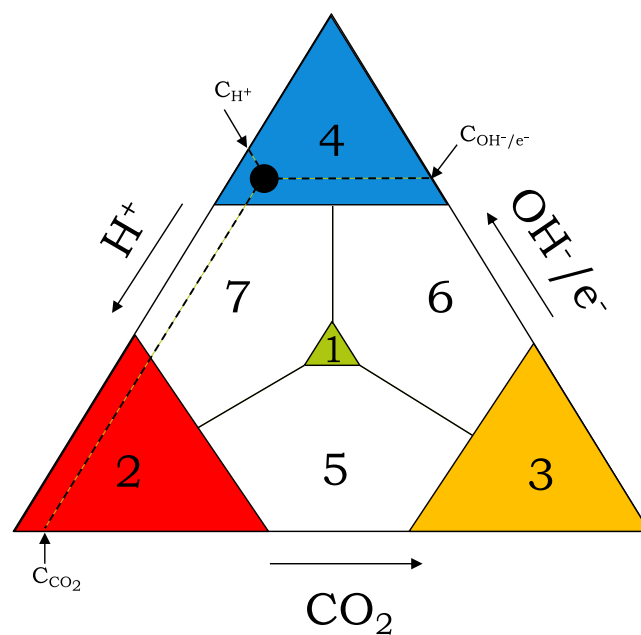

Figure 4. Qualitative triangular schematic diagram to explain the FE for CO2R and (bi)carbonate formation in acidic media. Region 1 (green) has a correct CO_2, H^+, and e^- stoichiometry; region 2 (red) is deficient in CO_2 and electrons; region 3 (orange) is deficient in H^+ and electrons; region 4 (blue) is deficient in CO_2 and H^+; region 5 is deficient in electrons; region 6 is deficient in H^+; and region 7 is deficient in CO_2. The axes represent the concentrations of CO_2, electrons, and protons on a reaction site of the electrode. The point in region 4 has a low concentration of CO_2 and protons and a high concentration of hydroxides, which will cause (bi)carbonate formation. See the main text for an explanation of other regions.

regions are arbitrarily chosen, but they could be quantitatively determined by computational or experimental means. In this diagram, there is a small operating window (region 1 in Figure 4) where protons, electrons/hydroxides, and CO_2 are correctly balanced resulting in high FEs and no (bi)carbonate formation. Note that hydroxide generation is correlated with the number of electrons according to reaction R1. Region 2 has an excess

of protons (i.e., deficient in CO_2 and electrons/hydroxides), which will cause the HER. Region 3 is deficient in protons and electrons/hydroxides, which corresponds with a state that is limited by kinetics. Region 4 has an excess of hydroxides (i.e., deficient in protons), which will cause (bi)carbonate formation. Region 5 is deficient in electrons/hydroxides and has an excess of protons (HER region). Region 6 is deficient in protons ((bi)carbonate formation region), and region 7 is deficient in CO_2 (mass transport limitation). Therefore, the key for suppressing HER and (bi)carbonate formation in acidic media is to find the operating conditions that comply with the requirements of region 1 in Figure 4.[71−73] Clearly, efficient CO2R in acidic media relies on a proper understanding of both the CO2RR and the HER as a function of the reaction conditions (e.g., pH, temperature, pressure, electrolyte type and concentrations, etc.). In choosing the reaction conditions for CO2R in (slightly) acidic media, it is important to know the relative contributions of H^+ reduction and water reduction to the HER for a specific catalyst as a function of process variables like the pH and temperature.

Using highly acidic electrolytes has several consequences for the CO2R process. First, the neutralization of the hydroxides generated at the cathode with the acids will cause a potential drop, which can be estimated with a Nernst-like equation

$$V_{loss} \sim \frac{2.303RT}{nF}\log\left(\frac{[H^+]^{bulk}}{[H^+]^{cath}}\right) \approx 0.059\Delta pH \quad (1)$$

where R, T, n, F, $[H^+]^i$, and ΔpH are the ideal gas constant, (room) temperature, charge of a proton, Faraday's constant, concentration of protons in the bulk and at the cathode surface, and the pH difference between the bulk and the cathode surface, respectively. Assuming that the concentration of hydroxide ions at the cathode surface is 1 M (i.e., the pH is 14) and the pH of the surrounding bulk is around 1, the potential drop will be approximately 0.77 V. For this reason, the cell potential (energy requirements) for CO2R in acidic media is typically higher than in alkaline media.

The second drawback of performing CO2R in acidic media is the requirement of precious metals for the oxidation reaction, since most non-noble OER catalysts are unstable in acidic solutions. Efficient, stable, and affordable electrocatalysts for the OER should be developed for CO2R in acidic media.[74]

Third, the highly acidic electrolytes will cause corrosion in the reactor and downstream separation processes. Furthermore, using concentrated electrolytes will contaminate liquid products, which will require a costly separation step. For this reason, solid electrolytes should be used whenever possible, in particular, when liquid CO2R products are involved.

5.2. Bipolar Membrane Electrolyzer.
A bipolar membrane is formed by lamination of a cation exchange layer (CEL) and an anion exchange layer (AEL). The BPM can be operated in two modes; the forward bias mode when the AEL is facing the cathode and the CEL is facing the anode, and the reverse bias mode when the CEL and AEL are reversed with respect to the forward bias mode. Applying a sufficiently high voltage in the reverse bias mode will cause water splitting at the CEL-AEL interface of the BPM, see Figure 5. The produced protons and hydroxide ions will migrate through the CEL and AEL toward the cathode and anode, respectively. The hydroxide ions will be oxidized at the anode, while the protons will neutralize the hydroxides and (bi)carbonates generated at the cathode from CO2R or participate in the
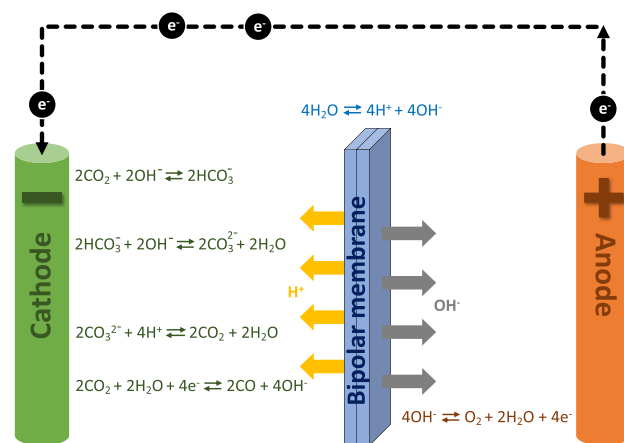

Figure 5. Bipolar membrane-based electrolysis of CO_2. Formed (bi)carbonates are neutralized with the protons from water splitting at the BPM junction. The BPM is operated in the reverse bias mode.

HER. BPM-based electrolyzers can also be used to regenerate CO_2 from reactive solutions, but this will be discussed in a later section. Under the forward bias mode, the CEL facing the anode blocks the crossover of (bi)carbonate ions, which react with the protons from the OER to form CO_2 at the CEL-AEL interface. The AEL facing the cathode provides the desired local alkalinity for efficient CO2R. The drawback of operating in the forward bias mode, in particular, at high CDs, is the evolution of CO_2 at the BPM junction causing membrane blistering and delamination of the CEL and AEL. Nevertheless, both operation modes have been studied for CO2R and will be briefly discussed next.

We note that bipolar membranes were used in CO2R long before the carbonation problem was widely acknowledged. It has been used for maintaining the pH of the anode and cathode compartments, preventing product crossover, and acidification and basification without the addition of acids and bases. Here, we confined the discussion to studies that used BPMs, in particular, for preventing the carbonation effect.

Eriksson et al.[34] and Ma et al.[31] used a BPM-based flow cell in the reversed bias mode to study (bi)carbonate crossover during CO_2 electrolysis at high and low CDs, respectively. Both studies found that the (bi)carbonate crossover rate was significantly reduced when a BPM was used. For 0.1 M KOH as anolyte and 1 M $KHCO_3$ as catholyte, Eriksson et al.[34] found an almost 10 times lower CO_2 crossover rate at 45 mA/cm^2 when using a BPM compared to an AEM. Ma et al.[31] showed that, for a BPM-based cell the CO_2/O_2 ratio in the anodic gas mixture was 0.3 at a CD of 200 mA/cm^2. Yang et al.[75] used a BPM-based MEA (BPMEA) cell without a flowing catholyte to prevent parasitic CO_2 losses. These authors obtained a high CO_2 utilization (up to 60% for 3 M KOH) and 68% FE of CO at 50 mA/cm^2 and ~3.5 V by promoting cation (K^+) crossover from the anolyte through the BPM to the cathode surface. This cation-infused BPM system increased the FE of CO, the activity of CO_2 reduction, and the CO_2 utilization but did not completely eliminate CO_2 loss to (bi)carbonates. Due to charge neutrality constraints, the hydroxides generated from the CO2RR will combine with the cations transported from the anolyte and produce (bi)carbonates upon reaction with CO_2. In such a BPM configuration with alkali cation crossover, it is hard to completely eliminate CO_2 loss, even if the BPM is able to

provide sufficient protons, because the cations should combine with the hydroxides, as charge neutrality always prevails. Nevertheless, the work of Yang et al.[75] shows/confirms the importance of concentrating cations near the electrode surface to suppress the HER and to increase the CO2R activity in an acidic reaction environment. Note that BPMEA cells (i.e., BPM in direct contact with the cathode) typically result in excessive hydrogen evolution due to the highly acidic cation exchange layer (Nafion) of the BPM. For this reason, BPM-based cells typically use a thin buffer layer or an additional (weak acid) cation exchange layer.[76,77] Recently, Xie et al.[78] used an MEA with a stationary unbuffered catholyte layer (SUCL) between the BPM and the cathode to in situ convert (bi)carbonate to CO_2 and to promote CO2R to C_{2+} products. The SUCL consisted of a porous poly(vinylidene fluoride) (PVDF) support saturated with a concentrated electrolyte. Using the SUCL-BPMEA cell, Xie et al.[78] obtained an anodic CO_2/O_2 ratio of 0.06 at 200 mA/cm^2 corresponding with a single-pass CO_2 utilization (SPU) of 78%, which overcomes the SPU limit of an AEM-based cell of 25% for multicarbon products. The performance of the cell could be controlled by the thickness of the SUCL, the type and concentration of the support electrolyte, using a water-dissociation catalyst between the AEL and CEL of the BPM, and the CO_2 flow.

Pǎtru et al.[79] used a BPM-based MEA to study carbon crossover during CO2R to CO on a gold catalyst. The BPM was operated in the forward bias mode (i.e., the alkaline side was facing the anode, while the acidic side was facing the anode). In this mode, two MEA configurations were tested. In the standard configuration, the alkaline side of the BPM was directly in contact with the cathode. In the novel configuration, an alkaline anion exchange layer was placed between the cathode and a CEM forming a BPM-like configuration in the forward bias mode. Note that, in both configurations, the anion exchange layer is facing the cathode, which provides a local alkaline environment that is beneficial for CO2R. In the standard configuration, the CO_2 crossover was significantly reduced, but not completely eliminated. However, this configuration suffered from delamination of the BPM due to the accumulation of water and CO_2 at the CEL-AEL interface. The novel configuration completely eliminated CO_2 crossover, but also suffered from stability issues related to cathode flooding due to accumulation of water. For both configurations, the obtained CO selectivities were lower than 15% at 50 mA/cm^2 with a feed of 50/50 vol % of CO_2/Ar and oxidizing pure H_2 at the anode. The main disadvantage of operating the BPM in the forward bias mode is that the oxidation reaction needs to be performed in acidic conditions, which requires expensive noble catalysts. However, as shown by Pǎtru et al.,[79] much higher CDs can be obtained in the forward bias mode than in the reverse bias mode at the same potential. The novel BPM configuration of Pǎtru et al.[79] is promising in eliminating CO_2 crossover, but requires proper CO_2 and water management in the cathode compartment to overcome stability issues.

5.3. Cascade CO$_2$ Electrolysis. The idea of the tandem/cascade process is to first convert CO_2 to CO, which is reduced in a second step to higher hydrocarbons, see Figure 6. The tandem/cascade concept can be performed either at the microscopic level by using a tandem catalyst that first converts CO_2 to CO,[80−82] which is further reduced on an adjacent active site to other products, or at the macroscopic level by using two separate reactors for both steps. We will focus on the
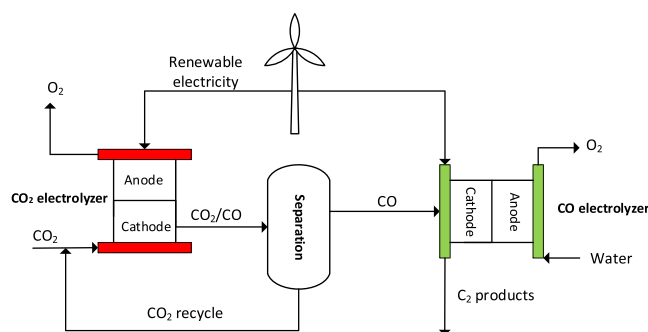

Figure 6. Cascade process for CO_2 electrolysis to hydrocarbons. In the first step, CO_2 is reduced to CO using a high-temperature SOEC process or a low-temperature acid-based process. In the second step, CO is reduced to higher hydrocarbons in alkaline media.

latter option, because on the microscopic level it is difficult to (1) independently control the reaction environment of both reactions, (2) separate the (unreacted) CO_2, and (3) find a stable tandem catalyst for the desired products. For the first CO2R step, the high-temperature SOEC process or the low-temperature process for CO_2 conversion to CO in acidic media can be used. The SOEC process does not suffer from the carbonation effect, while (bi)carbonate crossover in the low-temperature CO2R process is avoided if the reaction is performed in acidic media. The second CO reduction (COR) step can be performed in alkaline media, which is advantageous for C−C coupling, but without (bi)carbonate formation because CO does not react with hydroxides.[83] The drawback of performing the second step in alkaline media is the dissociation of acid products (e.g., acetate) from the COR reaction (CORR), which complicates the downstream separation. The choice between the low-temperature and high-temperature process for CO production depends on the advantages and disadvantages of both technologies.[84] The SOEC process operates at low cell voltages (∼1.0 V) and high temperatures (700−900 °C) and requires, in addition to electricity, also heat input. In terms of the energetic efficiency (EE) and the electric power consumption (EPC), the SOEC process is superior to the low-temperature process.[85] In addition, the SOEC process does not suffer from carbonate formation and achieves relatively high single-pass CO_2 conversions (up to 50%). At higher conversions, the SOEC process suffers from carbon deposition due to the Boudouard reaction ($2CO \leftrightarrow CO_2 + C$). The SOEC process for CO_2 conversion to CO has a high technology readiness level (TRL) as it is commercialized by Haldor Topsoe under the trade name eCOs.

The low-temperature (LT) process for CO2R to CO relies on finding a cost-effective solution to the carbonation problem. The LT process does not suffer from carbon deposition and could in theory achieve a higher single-pass conversion (SPC) than the SOEC process. The advantages of the LT process are its better suitability for high-pressure operation, integration with CO_2 capture processes, and ability to run in an intermittent mode. The SOEC process uses (pure) gaseous CO_2, while the LT process can utilize CO_2 capture solutions as well. However, the LT process will not be able to compete with the SOEC process in terms of EE and EPC due to thermodynamic constraints.

The second (COR) step of the cascade process can be performed in neutral or alkaline media without the carbonation

effect. Alkaline conditions are beneficial for C−C coupling and reduce the cell potential, but the drawback is that typical acidic CO2R products like acetic acid will dissociate into the ionic form, which are more difficult to recover. The use of alkaline electrolytes is less of an issue for gaseous products (e.g., ethylene) and for alcohols like ethanol and propanol. The conversion of CO to C_{2+} products in acidic media has yet to be explored, but promising results have been achieved in alkaline conditions. The challenges of COR to C_{2+} products are related to achieving high CDs, selectivities, energetic efficiencies, single-pass conversions, and stability. It is important to note that COR to C_{2+} products are only since recently being studied and the optimal process and reaction conditions still need to be optimized.

Ozden et al.[86] studied the cascade approach for carbonate-free CO2R to ethylene. For the first (CO2R) step, the high-temperature SOEC process was used for CO production. In the second step, CO was reduced to ethylene in an AEM-based MEA using a Cu-based catalyst coated with an *N*-tolyl-tetrahydro-bipyridine (Py) film to stabilize key reaction intermediates and a short-side chain (SSC) ionomer to enhance CO transport to the catalyst surface. These authors obtained in the first step a CO FE of 91%, and a CO_2-to-CO SPC of ∼45% at 815 mA/cm^2 and a cell voltage of ∼1.1 V for a CO_2 flow rate of 15 sccm, corresponding with an energy input of 13.49 GJ/ton CO. Using the Cu:Py:SSC catalyst and 3 M KOH catholyte for the second step, Ozden et al.[86] obtained an ethylene FE of 61% at 150 mA/cm^2 and ∼2.75 V for 110 h. These results show that the COR system outperforms the state-of-the-art CO2R reactor, in particular, when including the carbonation effect, in terms of ethylene FE, full cell EE, and stable operation duration. Ozden et al.[86] also tested an integrated system for CO_2 conversion to ethylene by combining the SOEC process for CO production with the CO-to-ethylene MEA reactor. Operating the SOEC at 800 °C and a CD of 550 mA/cm^2 yielded a CO FE of 95%, CO full-cell EE of 86%, and a SPC of 48%. The product mixture from the SOEC was purified with an amine solution to capture CO_2 before feeding to the COR reactor. The combined system produced ethylene at 120 mA/cm^2 and an MEA cell voltage of ∼2.4 V with a C_{2+} FE of 76% and a CO_2-to-ethylene SPC of 11%. The cascade system has an energy intensity of 138 GJ/ton ethylene, which compares favorably with the direct CO_2-to-ethylene conversion route (267 GJ/ton ethylene). Ozden et al.[86] further improved the energy efficiency of the MEA system by replacing the oxygen evolution reaction with the glucose oxidation reaction (GOR). These authors obtained an ethylene FE of 55% at 120 mA/cm^2 and MEA cell voltage of 1.27 V, corresponding with a total energy requirement of the cascade system of 89 GJ/ton ethylene. This shows the potential of energy savings by smart system integration and reactor configurations.

Sisler et al.[87] evaluated the economics of CO_2 to ethylene conversion in a neutral MEA cell, an alkaline cell, and a cascade system. These authors showed that, even for a very low carbonate formation ratio (CFR) of 1:1 (CO_2 molecules lost/CO_2 molecules reduced), an energy efficiency of >65% is required for a cost-effective production of ethylene at $1000/ton with an optimistic electricity price of $20/MWh. The cost of ethylene for the MEA and alkaline cells was estimated using current lab data for cell voltages, FEs, EEs, CDs, SPCs, and CFRs to be, respectively, ∼6 and ∼8 times higher than the reference price of $1000/ton. Even the optimistic scenario

with significant improvements in the performance metrics of both cells resulted in a cost that was higher than the reference price of ethylene. For the cascade process, using current lab data, the cost of ethylene was estimated to be a factor three higher than the reference price of $1000/ton. However, in the optimistic scenario with significant improvements for the CO2R-to-CO and COR-to-ethylene steps, a competitive cost of ethylene (<$1000/ton) was obtained. The results of Sisler et al.[87] show that CO_2 electrolyzers with significant carbonate formation are unlikely to become economically viable. For this reason, the cascade process is the most promising system for carbonate-free and cost-effective ethylene production. This conclusion is in agreement with our recent analysis of the direct and indirect (cascade) routes of CO_2 conversion to C_2 products. We presented a detailed process design and techno-economic analysis of both conversion routes, including CO_2 capture, electrochemical conversion of CO_2/CO to C_2 products, and downstream separation. Our analysis showed that both routes are not profitable under the base case scenario, which used state-of-the-art data for CO_2 and CO electrolyzers. For the best case scenario, which entails marginal improvements in the cell voltage (<2.5 V for CO-to-C_2), capital cost of the electrolyzers (<$10 000/m^2)), and the electricity price (<$20/MWh), resulted in a positive net present value (NPV) for both routes. Overall, the indirect (cascade) route was shown to have a greater potential for scale-up than the direct (single-step) route for CO_2 conversion to C_2 products. The performance and economics of the cascade process can be improved by increasing the SPC and reducing the temperature of the SOEC, increasing the CD for CO-to-C_{2+} conversion at low overpotentials, suppressing the HER, and replacing the OER with a more efficient oxidation reaction in the second (COR) step.

5.4. Electrolysis of Reactive Carbon Solutions. The success of gas-fed CO_2 electrolyzers relies on finding a cost-effective solution to the carbonation phenomena, but if this remains elusive, electrolysis of reactive carbon solutions (e.g., (bi)carbonate and amine) might provide an alternative to gaseous CO2R. It is important to emphasize that the concept of CO_2 electrolysis to useful products builds upon the implicit assumption that dilute carbon streams can be utilized. So far, efficient CO2R has been demonstrated for relatively concentrated CO_2 streams. This essentially means that, prior to the electrolysis step, CO_2 needs to be captured from a dilute source and regenerated to obtain a concentrated stream. Obviously, the initial aim of the CCU concept was to avoid, a priori, the costly regeneration step. (Bi)carbonate electrolyzers have the potential to eliminate the CO_2 regeneration/stripping step. CO_2 from dilute sources can be captured with alkaline electrolytes (e.g., KOH) to produce (bi)carbonates, which can be converted in a liquid-fed electrolyzer to useful products. To the best of our knowledge, (bi)carbonates are not directly reduced to CO2R products but first in situ converted to CO_2 (according to (R7) and (R8)) using a CEM or BPM-based electrolyzer.[88] The in situ generated CO_2 is then reduced to the desired products. However, as shown by Marcandalli et al.,[69] bicarbonate can directly be reduced to hydrogen according to the following equation.

$$2HCO_3^- + 2e^- \leftrightarrow H_2 + 2CO_3^{2-} \tag{R15}$$
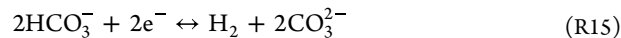
As noted by Marcandalli et al.,[69] cations must play an important role in the reduction of bicarbonate, which is negatively charged and would otherwise be repelled from the

cathode. Clearly, bicarbonate can act as a proton donor for the HER and limit the FE for CO2R. Important work in the field of (bi)carbonate electrolysis to CO, formate, and methane has been performed in the Berlinguette group.[89−92] Li et al.[89,90] used a BPM-based flow cell to convert a 3 M $KHCO_3$ solution to CO and formate. These authors obtained an FE for CO of 81% at 25 mA/cm^2 and 37% at 100 mA/cm^2. For formate, an FE of 64% at 100 mA/cm^2 and ~4 V was obtained. Gutiérrez-Sánchez et al.[93] used a BPM-based zero-gap flow electrolyzer to study the conversion of bicarbonate to formate. The effects of different operating parameters (CD, concentration and flow rate of bicarbonate, and temperature) on the FE of formate, the product concentration, the cell voltage, and energy efficiency were evaluated. A high energy efficiency of 27% was achieved for a CD of 50 mA/cm^2, a high concentration and flow rate of the electrolyte, and at room temperature. A high CD (>300 mA/cm^2) and a low flow rate were more beneficial for the downstream process, since the formate product stream was more concentrated, but at an expense of a lower energy efficiency. Lees et al.[91] used a BPM-based flow cell and a Cu cathode to convert bicarbonate (3 M $KHCO_3$) to methane. By adding a cationic surfactant to the catholyte that suppressed the HER, these authors obtained an FE of 27% and a yield of 34% for methane at a CD of 400 mA/cm^2 and cell voltage of 7.2 V. Recently, Zhang et al.[92] used a CEM-based flow cell coupled with the hydrogen oxidation reaction (HOR) at the anode to convert a 3 M $KHCO_3$ solution into CO. These authors reported a partial CD of CO of 220 mA/cm^2 and a CO_2 utilization efficiency of 40% at a cell voltage of 2.3 V, which is substantially lower than a BPM-based cell. Note that the standard potential of the HOR is 0 V, while that of the OER is 1.23 V.

Carbonate electroreduction in a BPM-based electrolyzer was studied by Li et al.[94] Using a silver catalyst, these authors produced syngas with a H_2/CO ratio of 3:1 at a CD of 150 mA/cm^2 and 3.8 V. The carbonate-to-syngas system was shown to be stable for a continuous run of 145 h. No CO_2 was detected in the syngas product, because all the in situ generated CO_2, from the reaction of carbonates with the protons of the BPM, was consumed by the CO2RR. Recently, Xiao et al.[95] studied the conversion of carbonate to pure syngas using a CEM-based flow cell and a CO_2 diffusion layer (CDL) inserted between the CEM and the cathode. These authors obtained a H_2/CO ratio of 1.2, corresponding to a CO FE of 46%, at 200 mA/cm^2 and ~3.7 V. Long-term stability tests at 100 mA/cm^2 and ~3.4 V showed stable operation and syngas production with a H_2/CO ratio of 2:1 for 23 h of experiments. The FE of CO (thus the H_2/CO ratio) could be controlled by the thickness of the CDL, the CD, and carbonate flow rates. Gutiérrez-Sánchez et al.[96] studied CO_2 conversion from direct air capture (DAC) solutions. A bench-scale DAC setup was used to capture CO_2 with a 1 M KOH solution to produce (bi)carbonate, which was converted to formate or CO in a BPM-based electrolyzer. The DAC solution contained a mixture of bicarbonate (~0.17 M) and carbonate (~0.49 M) after 8.5 h of CO_2 absorption from air. Gutiérrez-Sánchez et al.[96] obtained an FE of 16% and 13% at roughly 3.5 V for formate and CO, respectively. These FEs are significantly lower than state-of-the-art (bi)carbonate electrolyzers, which was attributed to the low concentration of (bi)carbonate in the DAC solution. Nevertheless, carbonate reduction seems to be more challenging than bicarbonate, due to the higher stability of the former, which requires more effort (i.e., it requires more heat and protons) to be decomposed to CO_2.

It is clear from the foregoing discussion that (bi)carbonate reduction is more challenging than CO2R. The reduction of (bi)carbonates requires a much higher cell voltage, in particular, when BPM-based cells are used, and yields lower FEs for the products due to the competing HER at increased potentials. More problematic is the observation that high (bi)carbonate concentrations are required for efficient electrolysis, which might not be attainable in a real CO_2 capture plant. Furthermore, in practice it is hard to obtain only bicarbonate or carbonate, since the species distribution in an alkaline (hydroxide) solution is governed by the acid−base equilibria, which is affected by the CO_2 loading.

A limited number of studies is available for electrochemical conversion of CO_2 from other reactive solvents (e.g., amines and ammonia). Lee et al.[97] studied the electrochemical conversion of CO_2 from amine solutions (monoethanolamine). These authors obtained an FE of 72% for CO at 50 mA/cm^2 by concentrating alkali cations near the electrode surface and (slightly) elevating the temperature. Liu et al.[98] investigated CO_2 electrolysis to formate using reactive ammonia solutions. Ammonia and CO_2 were reacted to form ammonium bicarbonate, which was fed to the electrolyzer to convert in situ generated CO_2 to formate. Different membranes (CEM, AEM, and BPM) were tested, but the cell configuration with an AEM was the most effective. The decomposition of ammonium bicarbonate was achieved by slightly increasing the temperature (40 °C). These authors obtained an FE of 85% for formate at a CD of 100 mA/cm^2 and 2.4 V outperforming state-of-the-art $KHCO_3$-fed electrolyzers. The higher efficiency for CO_2 conversion to formate from ammonium bicarbonate solutions was attributed to its lower decomposition temperature (~36 °C) compared to potassium bicarbonate (~150 °C).

We emphasize that care must be taken in selecting the reactive systems. For example, the species distribution for amines, ammonia, and hydroxide solvents depends on the reaction mechanism and CO_2 loading (mol CO_2/mol solvent).[99] Primary and secondary amines produce carbamate at low CO_2 loadings, while tertiary amines only form (bi)carbonates.[100−102] At high loadings, (bi)carbonates can be produced for primary and secondary amines as well. In the chilled ammonia process, ammonium bicarbonate, ammonium carbonate, ammonium carbamate, and sesquicarbonate can be formed depending on the temperature and CO_2 loading.[103,104] Ammonium carbamate is formed at low loadings and temperatures (<100 °C), while ammonium carbonate is formed at low temperatures (<50 °C) and intermediate loadings. Ammonium bicarbonate is mostly formed at high loadings, and sesquicarbonate is formed at intermediate loadings and temperatures. The reader is referred to Darde et al.[103,104] for the phase diagram of the different species as a function of temperature and loading. For aqueous hydroxide solvents (e.g., KOH and NaOH), carbonates and bicarbonates are formed at low and high CO_2 loadings, respectively.[105] In practice, it is difficult to exactly control the loading in CO_2 capture plants, because the loading is affected by several parameters (temperature, pressure, solvent type and concentration, CO_2 feed concentration and impurities, and the desired working capacity).

In summary, the chemical speciation during CO_2 capture with reactive solvents depends highly on the CO_2 loading,

which should be clearly defined/set in electrochemical experiments. Furthermore, the selection of reactive systems for electrochemical experiments should be based on practical CO_2 capture conditions (e.g., loading, temperature, etc.). Typically, CO_2 capture plants are not operated at the highest loading, because the reaction rate of CO_2 is higher (lower) at lower (higher) loadings, which reduces (increases) the length of the absorption column. As a consequence, carbamate or carbonate species are predominantly produced in the chilled ammonia and (primary and secondary) amine-based processes, while mainly carbonates are produced in the hydroxide-based systems. There is plenty of information available on CO_2 capture from which electrochemists can and should benefit to design efficient integrated capture and conversion processes.

5.5. In Situ CO_2 Recovery. It is possible to directly feed the anodic mixture to the cathode if the CO2RR is not much affected by the presence of O_2 (i.e., a lower partial pressure of CO_2), and if the product is a liquid. However, gaseous products will be contaminated with the O_2 that is retained in the gas phase. It is much easier to separate the anodic binary CO_2/O_2 mixture than a complex cathodic mixture containing, for example, unreacted CO_2, H_2, O_2, CO, CH_4, and ethylene. The presence of O_2 might also initiate unwanted oxidation reactions. Therefore, oxygen contamination of gaseous cathodic products should be avoided whenever possible.

We will now briefly discuss the proposed in situ CO_2 recovery and recycling methods. Note that a BPM-based electrolyzer can be used for in situ CO_2 recovery, but this was discussed in an earlier section and will not be repeated here. A three-compartment cell can be used to regenerate (bi)-carbonate in the center compartment; see, for example, Yang et al.[106] As shown in Figure 7, the cell is configured as (anode | CEM | AEM | cathode) to form the anode compartment, the center compartment, and the cathode compartment. In the center compartment, (bi)carbonates generated at the cathode are combined with the protons from the anode to produce CO_2 and water. The three-compartment cell is essentially a combination of an electrolyzer and an electrodialyzer. The drawbacks of the three-compartment cell are the higher cell voltage and cost due to the presence of an additional compartment, the evolution of CO_2 in the center compartment causes potential drop, and the low conductivity in the center compartment, which can be overcome by using conductivity promoters such as ion-exchange resin beads or solid electrolytes.

Recently, Kim et al.[107] used a three-compartment reactor with a porous solid electrolyte in the center compartment to regenerate CO_2 from (bi)carbonates produced at the cathode during CO2R to CO. These authors demonstrated up to 90% recovery of the crossover CO_2, while delivering an almost pure CO_2 stream, and over 90% FE of CO at 200 mA/cm^2.

Xie et al.[108] reported a very clever strategy to avoid the CO_2/O_2 separation of the anodic gas. These authors combined the CO2RR at the cathode with the glucose oxidation reaction (GOR) at the anode to almost completely eliminate the OER. The electrochemical oxidation of glucose consumed the hydroxide ions to produce gluconic acid.

$$C_6H_{12}O_6 + 2OH^- \rightarrow C_6H_{12}O_7 + H_2O + 2e^- \qquad (R16)$$
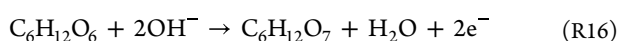
The main product of the electrochemical oxidation of glucose was gluconic acid, but other byproducts such as glucaric acid and guluronic acid were produced as well.[109] The disadvantages of this concept are related to the byproduct formation
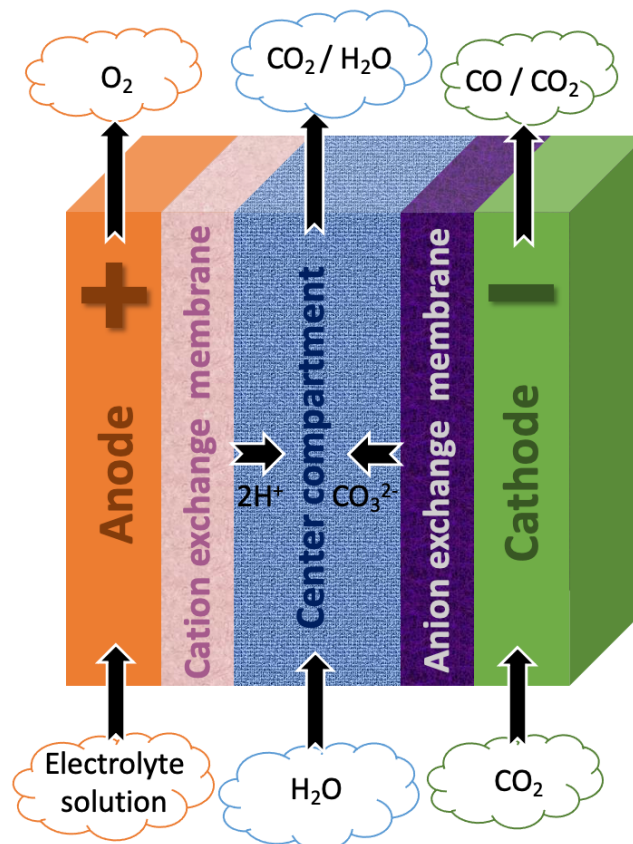

Figure 7. Three-compartment cell for in situ regeneration of CO_2 from (bi)carbonates. Protons from the anode and (bi)carbonates from the cathode are transported through the cation exchange membrane and the anion exchange membrane, respectively. The protons and (bi)carbonates combine in the center compartment to produce water and CO_2, which can be recycled to the cathode.

and the dissociation of the acid into the conjugate base form due to the operation in alkaline conditions. This will require a complicated downstream acidification and separation to obtain the desired market products. Nevertheless, Xie et al.[108] showed that almost pure CO_2 can be obtained at the anode by the elimination of oxygen evolution from the oxidation of hydroxide ions, which were locally consumed by the GOR.

O'Brien et al.[110] used a CEM-based MEA cell with a permeable CO_2 regeneration layer (PCRL) to enable a single-pass CO_2 conversion of 85% by locally regenerating CO_2 from (bi)carbonates. The cathode was spray-coated with an anion exchange ionomer solution to produce the PCRL. This layer creates locally an alkaline environment that suppress the HER, while enabling (bi)carbonate regeneration from the CO2RR with protons from the anode. The CO_2 and water produced at the PCRL-CEM interface from the neutralization reaction are transported to the catalyst by diffusion through the water-filled ionic domains of the polymer. The membrane in the study of O'Brien et al.[110] was thin to minimize the obstruction of CO_2 and water transport to the catalyst. Note that a poor transport will cause delamination of the layers like in a BPM or cause cathode flooding.

5.6. Ex Situ CO_2 Recovery. A range of technologies (e.g., absorption, adsorption, and membranes) are available to capture CO_2 from the anodic stream.[111] The choice of technology and the associated costs depend on the partial

pressure of CO_2 in the feed and the desired purity and/or recovery.[112] The partial pressure of CO_2 in the anodic gas mixture is relatively high (similar to biogas streams), which means that all the above-mentioned technologies could be applied to remove CO_2.[113] In this case, the required purity and recovery will determine the technology of choice. Adsorption and membrane-based processes show a trade-off between purity and recovery and cannot be used if high purities and recoveries are required.[114,115] We note that CO_2 and O_2 have very similar kinetic diameters, which presents a challenge for separations that are purely based on size exclusion (e.g., adsorption).[116,117] Absorption with selective chemical or physical solvents can be used to obtain high CO_2 purities and recoveries. As discussed earlier, low-purity CO_2 (i.e., contaminated with O_2) can be used at the cathode if the CO2RR is not much affected by the partial pressure of CO_2 and for liquid CO2R products, since O_2 will mostly be retained in the gas phase. For CO_2 conversions <100% and in the absence of gaseous CO2R products and hydrogen, the outlet gas from the cathode will contain unreacted CO_2 and O_2, which needs to be separated or purged to prevent buildup of inerts. In this case, the separation of the cathodic CO_2/O_2 mixture is similar to the separation of the anodic CO_2/O_2 mixture, but the separation cost can be different due to differences in the CO_2 concentration of both mixtures.

Sarswat et al.[118] proposed a simple strategy to bypass the separation of the anodic CO_2/O_2 mixture by combusting it with methane to produce pure CO_2, which can be recycled to the electrolyzer. The heat generated from the combustion can be used to drive other downstream separation processes (e.g., acetic acid distillation). This looks like an elegant solution, but the drawback is that it adds more CO_2 to the cycle due to the combustion of methane. However, the use of this solution makes sense as long as the separation processes are not (or cannot be) fully electrified.

5.7. Electrolyte Recovery. An additional downside of CO2R in alkaline media is the carbonation of the electrolyte, which needs to be regenerated in the long run. For example, potassium hydroxide as catholyte and/or anolyte will be converted to potassium (bi)carbonate during CO2R. The carbonation of the electrolyte is undesired, because it causes pH changes of the anolyte and/or catholyte, which in turn affect the CO2RR, and the conductivity is reduced (i.e., the ohmic losses increase). Different technologies are available to regenerate carbonated electrolytes. We will briefly discuss the bipolar membrane electrodialysis (BPMED) process reported by Eisaman et al.[119,120] and the double-loop process of Keith et al.[121] for CO_2 regeneration and electrolyte recycling.

Eisaman et al.[119] used a BPM-based electrodialysis stack to regenerate CO_2 from $KHCO_3$ and K_2CO_3 solutions. In the BPMED unit, CEMs, BPMs, and AEMs were alternately stacked to form the base, acid, and feed compartments. The protons and hydroxides generated by water splitting at the BPM are used to perform acid–base reactions, which produce CO_2 and KOH in the acid and base compartments, respectively. These authors showed that the energy requirement for CO_2 regeneration from 0.5 M $KHCO_3$ and 0.5 M K_2CO_3 solutions are roughly 100 and 200 kJ/mol CO_2 in the low-CD regime. The energy requirement increased almost linearly with increasing CD, and decreased with increasing pressure, which reduced the ohmic losses by suppressing bubble formation in the stack relative to ambient-pressure operation. A very important conclusion from the work of

Eisaman et al.[119] is that CO_2 and KOH regeneration from $KHCO_3$ is almost two times more energy efficient than from K_2CO_3.

Keith et al.[121] designed a double-loop process to capture CO_2 from the atmosphere using a KOH solution and to regenerate the CO_2 and the alkali solution from the formed K_2CO_3 solution. In the first loop, CO_2 is captured with a KOH solution to form K_2CO_3. In the second loop, the carbonate ions are precipitated with calcium forming $CaCO_3$, which is calcined to produce CO_2 and CaO. The CaO is hydrated in a slaker to produce $Ca(OH)_2$, which is combined with K_2CO_3 from the first loop to produce KOH and $CaCO_3$ to close the loops. The disadvantage of the process is the relatively high complexity, capital cost, and energy requirements, which can be reduced significantly by proper heat integration. The total energy consumption of the process was reported to be 8.8 GJ of natural gas per ton of CO_2 captured and delivered at 150 bar. The energy consumption for CO_2 capture from flue gas and solvent (monoethanolamine) regeneration is roughly half of the double-loop process (~4 GJ/ton CO_2 delivered at 150 bar). Note that the difference in energy requirements is mainly due to the differences in the CO_2 concentration of both feeds (400 ppm (ppm) for direct air capture vs 10 v% for flue gas). The double-loop process is currently being up-scaled and commercialized by Carbon Engineering for direct air capture.

6. ECONOMICS OF CO_2 AND ELECTROLYTE RECYCLING

It is clear that the carbonation phenomena will bring additional costs for CO_2 and electrolyte recycling. The cost of CO_2 capture depends on the concentration of CO_2 in the feed. The cost of CO_2 removal from the anodic mixture containing 80%, 66.6%, and 50% of CO_2 can be estimated with the Sherwood correlation (cost vs concentration curve) of Bains et al.[122] to be $16/ton, $18/ton, and $21/ton, respectively. These costs are in the range of CO_2 capture from natural gas and biogas, which also have high CO_2 concentrations in the feed. Note that this is only the cost of CO_2 capture and recycling from the anodic stream. The gas stream from the cathode requires separation as well if gaseous CO2R products and/or hydrogen is produced and the conversion of CO_2 is <100%. The cost of CO_2 capture from the cathodic stream depends on the single-pass conversion, but this is typically <25%, which means that the concentration of (unreacted) CO_2 in the outlet is relatively high. Under these conditions, we expect a similar cost of merit for CO_2 capture from the cathode and anode streams.

The costs of electrolyte recycling can be estimated from the data of Eisaman et al.[119] for the BPMED process and Keith et al.[121] for the double-loop DAC process. As an example, we assume that 1 M KOH has carbonated to 0.5 M K_2CO_3 in the CO_2 electrolyzer according to

$$2KOH + CO_2 \leftrightarrow K_2CO_3 + H_2O \qquad (R17)$$
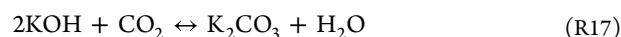
Using the energy consumption of 200 kJ/mol (or 0.055 kWh/mol) of CO_2 from Eisaman et al.[119] and assuming an electricity price of $50/MWh, the cost can be estimated as $63/ton of CO_2 or ~$20/ton of K_2CO_3 or ~$50/ton of KOH. Note that this only includes the electricity cost (i.e., the capital cost is excluded). The cost can be lowered significantly by reducing the power consumption (i.e., the cell voltage) and the electricity price.

The cost of CO_2 and KOH recycling using the double-loop process of Keith et al.[121] can be estimated from the energy

consumption of 8.8 GJ of natural gas per ton of CO_2 (or 8.3 GJ/ton if we subtract 0.5 GJ/ton for the compression) and a natural gas price of $10/GJ to be $83/ton of CO_2 or ~$65/ton of KOH. Again, these costs only include the operational expenditures. Clearly, the double-loop process is slightly more expensive than the BPMED process, but the cost highly depends on the price of heat (natural gas), which is currently very high due to geopolitical issues.

It is clear from the foregoing discussion that the carbonation effect will significantly contribute to the cost of the CO2R product. As an example, we calculated the cost of CO2R to CO in the absence or presence of the carbonation phenomena for three reactor configurations (full MEA, flow cell, and SOEC), see Table 1. In the calculations, we assumed a capacity of 1

Table 1. Estimation of Total Costs for 1 ton/h of CO_2 Conversion to CO in a MEA, Flow Cell, and SOEC

Cost estimation	MEA	flow cell	SOEC
Cell voltage (V)	2.5	2.5	1.2
CD (mA/cm^2)	250	250	500
Faraday efficiency (%)	100	100	100
Single-pass CO_2 conversion (%)	25	25	50
CO_2 electrolyzer ($/ton CO)	279	279	134
CO_2 purchase ($/ton CO)	79	79	79
CO_2 capture cathode ($/ton CO)	56	56	33
CO_2 capture anode ($/ton CO)	28	0	0
Electrolyte recycling ($/ton CO)	0	99	0
Total ($/ton CO)	442	513	245

ton/h of CO_2 conversion to CO, a CO_2 purchase price of $50/ton, 8000 h/y of operation, and a lifetime of 15 years. For the MEA and flow cell, we assumed that the FE of CO is 100%, the CD is 250 mA/cm^2 at a cell voltage of 2.5 V, and the mole conversion of CO_2 is 25%, which is the actual amount of CO_2 in moles that is converted to CO excluding the loss due to the carbonation phenomena. For the SOEC, we assumed an FE of 100%, a CD of 500 mA/cm^2 at a cell voltage of 1.2 V, and an SPC of 50%. For the MEA, we assumed that the hydroxides generated at the cathode react with CO_2 to produce carbonate, which crosses over to the anode and oxidizes to CO_2 producing a CO_2/O_2 ratio of 2:1. The MEA cell only requires CO_2 capture at the anode and cathode, but electrolyte regeneration is not needed, since alkaline electrolytes are not used in this reactor configuration. The correlation of Bains et al.[122] is used for the cost of CO_2 capture from the anode and cathode streams. We assumed that all lost CO_2 can be recovered such that only the fraction that is converted to CO needs to be purchased. For the flow cell, we assumed a carbonation ratio of 1 (i.e., for every mol of CO_2 reduced one mol of carbonate is produced). For alkaline electrolytes (e.g., KOH), we know from the crossover experiments that the electrolyte is first carbonated before CO_2 is released at the anode. This means that the electrolyte in a flow cell needs to be regenerated, but CO_2 capture at the anode is not needed if the electrolyte is continuously refreshed. The BPMED process of Eisaman et al.[119] is used for electrolyte recycling. Only the operating cost of the BPMED process was considered in the economic evaluation (the capital cost was neglected). The capital cost of all electrolyzers and the electricity price are assumed to be $1000/kW and $50/MWh, respectively. Depreciation, taxes, inflation, and maintenance are neglected in the cost calculations.

The required power of the electrolyzers was computed from

$$P_j = i_j \times A \times V \tag{2}$$

where P_j is the power required to produce component j, i_j is the partial CD for component j, A is the electrode area, and V is the cell voltage. The electrode area (A) required to convert 1 ton/h of CO_2 was estimated from[123]

$$A = \frac{n_j \times N_{CO_2} \times F}{i_t \times FE_j} \tag{3}$$

where N_{CO_2} is the mole flow of CO_2, i_t is the total CD, F is the Faraday constant, FE_j is the Faraday efficiency for component j, and n_j is the number of electrons involved in the CO2RR (2 for CO2R to CO).

In Table 1, the results of the economic analysis are presented. From these results, it is clear that the MEA and flow cell processes are a factor ~2 more expensive than the SOEC-based process for CO_2 conversion to CO. The low SPC and the CO_2 crossover in the MEA process significantly increase the cost of CO_2 capture. In the case of the flow cell, the low SPC and the carbonation of the electrolyte and its regeneration increase the cost. The SOEC is superior to the MEA and flow-cell-based processes due to its lower power consumption and higher SPC. Note that we have neglected the heat input of the SOEC, which typically has a minor contribution to the overall cost. Ozden et al.[17] provide an energy assessment of CO2R to ethylene for different cell configurations (alkaline flow cell, neutral MEA, BPMEA, cascade, and CO2R from reactive liquids). These authors also demonstrate that the SOEC-based cascade process is superior to the other cell configurations considering current performance data. However, the SOEC process is only developed for CO production; hence, we have to rely on CO2R or COR for C_{2+} products.

7. OUTLOOK

The scale-up of low-temperature CO_2 electrolyzers relies on a cost-effective solution for the carbonation problem. Although recent work has shed some light on the formation and crossover of (bi)carbonates during CO2R, the problem is more complex than initially expected and requires far greater research efforts to better understand and prevent bi(carbonate) formation, transport, and oxidation/neutralization at the anode. To address these challenges, it is crucial to align research across multiple disciplines, levels (fundamental and applied), and scales (micro to macro). In the following, we propose a list of research directions to tackle or deal with the carbonation problem.

- Anode: CO2R studies have mostly focused on the cathode, but the crossover phenomena demands more attention to the anodic processes.[124,125] The exact mechanism for CO_2 evolution (e.g., (bi)carbonate oxidation or neutralization) at the anode is still unclear. Also, it can be interesting to investigate the possibility to convert the (bi)carbonates to some useful products at the anode (e.g., carbonate esters).[126]

- Reactor design and configuration: The type and configuration of the reactor (flow cell, zero-gap MEA, and hybrid flow-MEA with CEM, AEM, or BPM) can have a huge influence on the carbonation phenomena. Clever cell designs will help minimize (bi)carbonate

formation, crossover, and CO_2 loss. The carbonation phenomena has mostly been studied in flow cells or hybrid cells, but the effects might be different for full MEA cells.[127−130]

- In situ measurements: At a fundamental level, more insights are required to better understand the underlying processes of (bi)carbonate formation, transport, and oxidation/neutralization. Probing the local (reaction) environment of the anode, cathode, and membrane using in situ/operando techniques will reveal the true nature of the carbonation phenomena.[65,66,131−134]

- Recycling: The separation of CO_2 from the anodic mixture is relatively easy due to the high concentrations, but it will add significantly to the cost if the single-pass conversion is low. Therefore, research should focus on in situ recycling methods (i.e., (bi)carbonate conversion to CO_2 inside the cell).

- Acidic media: CO2R has mostly been studied in alkaline media to suppress the HER. However, recent studies show that high FEs for CO2R can be achieved in (slightly) acidic media. The CO2RR will always locally generate hydroxides, because water instead of H^+ is involved in the mechanism. Therefore, research should focus on how to effectively neutralize the locally formed hydroxides and (bi)carbonates at the cathode, while suppressing the HER.

- Electrolysis of captured solutions: As discussed earlier, if a solution to the CO_2 crossover problem remains illusive, it is advantageous to design efficient liquid-fed electrolyzers based on reactive CO_2 capture solutions. In that case, CO_2 from a dilute source can be captured with an alkaline solution (e.g., amines, hydroxide, ammonia, etc.) and the formed (bi)carbonates and carbamates can be reduced to useful products (i.e., eliminating the costly CO_2 desorption step).[135,136]

- Membranes: Although different types of membranes (AEM, CEM, and PM) have been tested in CO_2 electrolysis, their role in (bi)carbonate rejection/crossover is poorly understood. The near-membrane environment can significantly be influenced by the type of membrane, which can affect the CO_2-bicarbonate-carbonate equilibria through water splitting and acid−base reactions with functional groups.[137−139]

- GDE design: The use of a GDE is crucial for high CD CO_2 electrolysis, but the carbonation effect causes flooding, which results in performance loss of the GDE. Creative GDE designs will be of paramount importance to overcome the flooding problem.[14,140]

- Multiscale/multiphysics modeling: CO2R at the electrode is a complex phenomenon that involves multiple phases (gas/liquid/solid) and reactions (homogeneous and heterogeneous), which are affected by the presence of electrolytes and electric field. Advanced modeling of the near-electrode and membrane environment will provide useful insights into the carbonation phenomena that is affected by mass transport, electrochemical and homogeneous reactions, and thermal effects.[141−145] Moreover, advanced thermodynamic modeling using electrolyte equations of state and molecular simulation are essential for predicting the key thermodynamic, transport, and structural properties of the relevant liquid systems.[146−148] Such properties are the mutual solubilities (e.g., gases in the aqueous electrolyte phase),

transport coefficients (i.e., Maxwell-Stefan and self-diffusivities, ionic conductivities, viscosity), and partial molar properties.[149−157]

- Electrolyte-free electrolysis: The presence of electrolytes in CO_2 electrolyzers has several disadvantages. First, liquid products are contaminated with the electrolytes, which complicate the downstream process. Second, cross-contamination of electrolytes will occur due to the use of different electrolytes in the cathode and anode compartments, and because membranes are not 100% selective. Third, CO2R in alkaline media not only cause carbon crossover but also the electrolytes are carbonated, which will require regeneration in the long term. For these reasons, the use of (liquid) electrolytes in CO_2 electrolyzers should be eliminated/minimized.[158−160]

- CO_2 capture: Although the carbonation effect is detrimental from a CO2R point of view, it presents opportunities for CO_2 capture and concentration. CO_2 from dilute sources can be transformed to (bi)carbonate at the cathode either during HER or CO2R and transported through the membrane and oxidized at the anode to produce higher concentrations of CO_2.[161−166] A theoretical CO_2 concentration of 80% or 67% can be achieved if bicarbonate or carbonate is the charge carrier, respectively.

- Experimental design: As a final note, we would like to stress that a careful design of experiments is important for the correct interpretation of results. The carbonation effect shows a complex time-dependent behavior, which is influenced by initial conditions (e.g., type, concentration and amount/flow of electrolyte, concentration and supply rate of CO_2, cell configuration, CD/cell voltage, time of measurements, position/location of the probes, etc.). For this reason, it is extremely important to specify all experimental details in publications. We encourage and hope that it will become a common practice to simultaneously measure/probe the anodic and cathodic processes.[167]

8. CONCLUSIONS

One of the most pressing problems in the field of low-temperature CO_2 electrolysis is the so-called carbonation phenomena, which is detrimental for the performance, economics, and scale-up of the process. The carbonation effect is a direct consequence of performing the CO2RR in neutral to alkaline media and the fact that water and not protons is involved in the mechanism, which essentially means that hydroxides are always generated at the cathode during CO2R. The parasitic reactions of CO_2 with the neutral/alkaline electrolytes result in (bi)carbonate precipitation and flooding in gas diffusion electrodes, CO_2 crossover to the anode, low carbon utilization efficiency, electrolyte carbonation and pH-drift in time, and additional cost for CO_2 and electrolyte recycling. In this review, we present a detailed discussion on the carbon crossover mechanism, the potential solutions for preventing/dealing with carbon crossover, the economics of CO_2 and electrolyte recycling, and an outlook for future research. A critical analysis of published results shows that the time-dependent behavior of the carbonation phenomena is affected by the CD and the initial conditions like the type, concentration, and flow of the electrolyte, the concentration and flow of CO_2, and the cell configuration (e.g.,

type of membrane, flow cell or MEA). The CO_2 to O_2 ratio at the anode is 4:1 for purely bicarbonate crossover, 2:1 for purely carbonate crossover, 1:1 for simultaneous crossover of one carbonate and two hydroxides, and 0:1 for CO2R in (highly) acidic media. Potential solutions for carbon crossover include (1) CO2R in acidic media, (2) CO2R with BPM-based electrolyzers, (3) cascade CO_2 electrolysis (e.g., CO_2-to-CO-to-hydrocarbons), (4) (bi)carbonate electrolysis, (5) in situ CO_2 recovery and recycling, and (6) ex situ CO_2 recovery and recycling. All these solutions will incur additional costs for the CO2R process, either due to a lower FE, a higher cell voltage, a higher investment, a lower CD, or a complex separation. The cost of CO_2 separation from the anodic mixture depends on the crossover rate and the concentration of CO_2, which is 80%, 66.6%, 50%, or 0% for, respectively, bicarbonate, carbonate, one carbonate plus two hydroxides, or only hydroxide, oxidation at the anode. The CO_2 capture cost is relatively low due to the relatively high concentrations of CO_2. However, the cost per ton of product will increase significantly for a low single-pass conversion and high crossover rate of CO_2. An additional downside of CO2R in alkaline media is the carbonation of the electrolyte, which requires a costly regeneration step. The carbonation phenomena is complex and requires research across multiple disciplines, levels, and scales with particular attention to anodic processes, reactor design, in situ measurements, CO_2 and electrolyte recycling, CO2R in acidic media, electrolysis of reactive solutions, membranes, GDE design, multiscale/multiphysics modeling, electrolyte-free electrolysis, and experimental design.

AUTHOR INFORMATION

Corresponding Author

Mahinder Ramdin − *Engineering Thermodynamics, Process & Energy Department, Faculty of Mechanical, Maritime and Materials Engineering, Delft University of Technology, 2628CB Delft, The Netherlands;* ◉ orcid.org/0000-0002-8476-7035; Email: m.ramdin@tudelft.nl

Authors

Othonas A. Moultos − *Engineering Thermodynamics, Process & Energy Department, Faculty of Mechanical, Maritime and Materials Engineering, Delft University of Technology, 2628CB Delft, The Netherlands;* ◉ orcid.org/0000-0001-7477-9684

Leo J. P. van den Broeke − *Engineering Thermodynamics, Process & Energy Department, Faculty of Mechanical, Maritime and Materials Engineering, Delft University of Technology, 2628CB Delft, The Netherlands*

Prasad Gonugunta − *Engineering Thermodynamics, Process & Energy Department, Faculty of Mechanical, Maritime and Materials Engineering, Delft University of Technology, 2628CB Delft, The Netherlands; Department of Materials Science and Engineering, Faculty of Mechanical, Maritime, and Materials Engineering, Delft University of Technology, 2628 CD Delft, The Netherlands*

Peyman Taheri − *Department of Materials Science and Engineering, Faculty of Mechanical, Maritime, and Materials Engineering, Delft University of Technology, 2628 CD Delft, The Netherlands*

Thijs J. H. Vlugt − *Engineering Thermodynamics, Process & Energy Department, Faculty of Mechanical, Maritime and Materials Engineering, Delft University of Technology,* 2628CB Delft, The Netherlands; ◉ orcid.org/0000-0003-3059-8712

Complete contact information is available at:
https://pubs.acs.org/10.1021/acs.iecr.3c00118

Notes

The authors declare no competing financial interest.

REFERENCES

(1) Ramdin, M.; Morrison, A. R. T.; de Groen, M.; van Haperen, R.; de Kler, R.; Irtem, E.; Laitinen, A. T.; van den Broeke, L. J. P.; Breugelmans, T.; Trusler, J. P. M.; Jong, W. d.; Vlugt, T. J. H. High-Pressure Electrochemical Reduction of CO_2 to Formic Acid/Formate: Effect of pH on the Downstream Separation Process and Economics. *Ind. Eng. Chem. Res.* **2019**, *58*, 22718−22740.

(2) Masel, R. I.; Liu, Z.; Yang, H.; Kaczur, J. J.; Carrillo, D.; Ren, S.; Salvatore, D.; Berlinguette, C. P. An industrial perspective on catalysts for low-temperature CO_2 electrolysis. *Nat. Nanotechnol.* **2021**, *16*, 118−128.

(3) Fan, L.; Xia, C.; Yang, F.; Wang, J.; Wang, H.; Lu, Y. Strategies in catalysts and electrolyzer design for electrochemical CO_2 reduction toward C2+ products. *Sci. Adv.* **2020**, *6*, eaay3111.

(4) Gawel, A.; Jaster, T.; Siegmund, D.; Holzmann, J.; Lohmann, H.; Klemm, E.; Apfel, U.-P. Electrochemical CO_2 reduction - The macroscopic world of electrode design, reactor concepts & economic aspects. *iScience* **2022**, *25*, 104011.

(5) Nitopi, S.; Bertheussen, E.; Scott, S. B.; Liu, X.; Engstfeld, A. K.; Horch, S.; Seger, B.; Stephens, I. E. L.; Chan, K.; Hahn, C.; Nørskov, J. K.; Jaramillo, T. F.; Chorkendorff, I. Progress and Perspectives of Electrochemical CO_2 Reduction on Copper in Aqueous Electrolyte. *Chem. Rev.* **2019**, *119*, 7610−7672.

(6) García de Arquer, F. P.; et al. CO_2 electrolysis to multicarbon products at activities greater than 1 A cm^{-2}. *Science (80-.)* **2020**, *367*, 661−666.

(7) Löwe, A.; Schmidt, M.; Bienen, F.; Kopljar, D.; Wagner, N.; Klemm, E. Optimizing Reaction Conditions and Gas Diffusion Electrodes Applied in the CO_2 Reduction Reaction to Formate to Reach Current Densities up to 1.8 A cm − 2. *Chem. Eng.* **2021**, *9*, 4213−4223.

(8) Ma, W.; Xie, S.; Liu, T.; Fan, Q.; Ye, J.; Sun, F.; Jiang, Z.; Zhang, Q.; Cheng, J.; Wang, Y. Electrocatalytic reduction of CO_2 to ethylene and ethanol through hydrogen-assisted C−C coupling over fluorine-modified copper. *Nat. Catal.* **2020**, *3*, 478−487.

(9) Gao, D.; Arán-Ais, R. M.; Jeon, H. S.; Roldan Cuenya, B. Rational catalyst and electrolyte design for CO_2 electroreduction towards multicarbon products. *Nat. Catal.* **2019**, *2*, 198−210.

(10) Wu, D.; Jiao, F.; Lu, Q. Progress and Understanding of CO_2/ CO Electroreduction in Flow Electrolyzers. *ACS Catal.* **2022**, *12*, 12993−13020.

(11) Haldor Topsoe, Produce your own Carbon Monoxide. https://www.topsoe.com/processes/carbon-monoxide, Accessed: 2023-01-09.

(12) Sunfire, Syngas: The renewable feed gas. https://www.sunfire.de/en/syngas, Accessed: 2023-01-09.

(13) Rabinowitz, J. A.; Kanan, M. W. The future of low-temperature carbon dioxide electrolysis depends on solving one basic problem. *Nat. Commun.* **2020**, *11*, 5231.

(14) Wakerley, D.; Lamaison, S.; Wicks, J.; Clemens, A.; Feaster, J.; Corral, D.; Jaffer, S. A.; Sarkar, A.; Fontecave, M.; Duoss, E. B.; Baker, S.; Sargent, E. H.; Jaramillo, T. F.; Hahn, C. Gas diffusion electrodes, reactor designs and key metrics of low-temperature CO_2 electrolysers. *Nat. Energy* **2022**, *7*, 130−143.

(15) Lees, E. W.; Mowbray, B. A. W.; Parlane, F. G. L.; Berlinguette, C. P. Gas diffusion electrodes and membranes for CO_2 reduction electrolysers. *Nat. Rev. Mater.* **2022**, *7*, 55−64.

(16) Yuan, L.; Zeng, S.; Zhang, X.; Ji, X.; Zhang, S. Advances and challenges of electrolyzers for large-scale CO_2 electroreduction. *Mater. Reports Energy* **2023**, *3*, 100177.

(17) Ozden, A.; García de Arquer, F. P.; Huang, J. E.; Wicks, J.; Sisler, J.; Miao, R. K.; O'Brien, C. P.; Lee, G.; Wang, X.; Ip, A. H.; Sargent, E. H.; Sinton, D. Carbon-efficient carbon dioxide electrolysers. *Nat. Sustain.* **2022**, *5*, 563−573.

(18) Jeng, E.; Jiao, F. Investigation of CO_2 single-pass conversion in a flow electrolyzer. *React. Chem. Eng.* **2020**, *5*, 1768−1775.

(19) Jing, X.; Li, F.; Wang, Y. Assessing the economic potential of large-scale carbonate-formation-free CO_2 electrolysis. *Catal. Sci. Technol.* **2022**, *12*, 2912−2919.

(20) Shin, H.; Hansen, K. U.; Jiao, F. Techno-economic assessment of low-temperature carbon dioxide electrolysis. *Nat. Sustain.* **2021**, *4*, 911−919.

(21) Li, M.; Irtem, E.; Iglesias van Montfort, H.-P.; Abdinejad, M.; Burdyny, T. Energy comparison of sequential and integrated CO_2 capture and electrochemical conversion. *Nat. Commun.* **2022**, *13*, 5398.

(22) Kötz, R.; Barbero, C.; Haas, O. Probe beam deflection investigation of the charge storage reaction in anodic iridium and tungsten oxide films. *J. Electroanal. Chem. Interfacial Electrochem.* **1990**, *296*, 37−49.

(23) Naito, T.; Shinagawa, T.; Nishimoto, T.; Takanabe, K. Recent advances in understanding oxygen evolution reaction mechanisms over iridium oxide. *Inorg. Chem. Front.* **2021**, *8*, 2900−2917.

(24) Patra, S. G.; Mizrahi, A.; Meyerstein, D. The Role of Carbonate in Catalytic Oxidations. *Acc. Chem. Res.* **2020**, *53*, 2189−2200.

(25) Liu, Z.; Yang, H.; Kutz, R.; Masel, R. I. CO_2 Electrolysis to CO and O_2 at High Selectivity, Stability and Efficiency Using Sustainion Membranes. *J. Electrochem. Soc.* **2018**, *165*, J3371−J3377.

(26) Kaczur, J. J.; Yang, H.; Liu, Z.; Sajjad, S. D.; Masel, R. I. Carbon Dioxide and Water Electrolysis Using New Alkaline Stable Anion Membranes. *Front. Chem.* **2018**, *6*, 1−16.

(27) Larrazábal, G. O.; Strøm-Hansen, P.; Heli, J. P.; Zeiter, K.; Therkildsen, K. T.; Chorkendorff, I.; Seger, B. Analysis of Mass Flows and Membrane Cross-over in CO_2 Reduction at High Current Densities in an MEA-Type Electrolyzer. *ACS Appl. Mater. Interfaces* **2019**, *11*, 41281−41288.

(28) Ma, M.; Clark, E. L.; Therkildsen, K. T.; Dalsgaard, S.; Chorkendorff, I.; Seger, B. Insights into the carbon balance for CO_2 electroreduction on Cu using gas diffusion electrode reactor designs. *Energy Environ. Sci.* **2020**, *13*, 977−985.

(29) Endrödi, B.; Kecsenovity, E.; Samu, A.; Halmágyi, T.; Rojas-Carbonell, S.; Wang, L.; Yan, Y.; Janáky, C. High carbonate ion conductance of a robust PiperION membrane allows industrial current density and conversion in a zero-gap carbon dioxide electrolyzer cell. *Energy Environ. Sci.* **2020**, *13*, 4098−4105.

(30) Mardle, P.; Cassegrain, S.; Habibzadeh, F.; Shi, Z.; Holdcroft, S. Carbonate Ion Crossover in Zero-Gap, KOH Anolyte CO_2 Electrolysis. *J. Phys. Chem. C* **2021**, *125*, 25446−25454.

(31) Ma, M.; Kim, S.; Chorkendorff, I.; Seger, B. Role of ion-selective membranes in the carbon balance for CO_2 electroreduction via gas diffusion electrode reactor designs. *Chem. Sci.* **2020**, *11*, 8854−8861.

(32) Haspel, H.; Gascon, J. Is Hydroxide Just Hydroxide? Unidentical CO_2 Hydration Conditions during Hydrogen Evolution and Carbon Dioxide Reduction in Zero-Gap Gas Diffusion Electrode Reactors. *ACS Appl. Energy Mater.* **2021**, *4*, 8506−8516.

(33) Lin, M.; Han, L.; Singh, M. R.; Xiang, C. An Experimental- and Simulation-Based Evaluation of the CO_2 Utilization Efficiency of Aqueous-Based Electrochemical CO_2 Reduction Reactors with Ion-Selective Membranes. *ACS Appl. Energy Mater.* **2019**, *2*, 5843−5850.

(34) Eriksson, B.; Asset, T.; Spanu, F.; Lecoeur, F.; Dupont, M.; Garcés-Pineda, F. A.; Galán-Mascarós, J. R.; Cavaliere, S.; Rozière, J.; Jaouen, F. Mitigation of Carbon Crossover in CO_2 Electrolysis by Use of Bipolar Membranes. *J. Electrochem. Soc.* **2022**, *169*, 034508.

(35) Zhong, H.; Fujii, K.; Nakano, Y.; Jin, F. Effect of CO_2 Bubbling into Aqueous Solutions Used for Electrochemical Reduction of CO_2 for Energy Conversion and Storage. *J. Phys. Chem. C* **2015**, *119*, 55−61.

(36) Moss, A. B.; Garg, S.; Mirolo, M.; Giron Rodriguez, C. A.; Ilvonen, R.; Chorkendorff, I.; Drnec, J.; Seger, B. In operando investigations of oscillatory water and carbonate effects in MEA-based CO_2 electrolysis devices. *Joule* **2023**, *7*, 350−365.

(37) Lu, X.; Zhu, C.; Wu, Z.; Xuan, J.; Francisco, J. S.; Wang, H. In Situ Observation of the pH Gradient near the Gas Diffusion Electrode of CO_2 Reduction in Alkaline Electrolyte. *J. Am. Chem. Soc.* **2020**, *142*, 15438−15444.

(38) Henckel, D. A.; Counihan, M. J.; Holmes, H. E.; Chen, X.; Nwabara, U. O.; Verma, S.; Rodríguez-López, J.; Kenis, P. J. A.; Gewirth, A. A. Potential Dependence of the Local pH in a CO_2 Reduction Electrolyzer. *ACS Catal.* **2021**, *11*, 255−263.

(39) Yang, K.; Kas, R.; Smith, W. A.; Burdyny, T. Role of the Carbon-Based Gas Diffusion Layer on Flooding in a Gas Diffusion Electrode Cell for Electrochemical CO_2 Reduction. *ACS Energy Lett.* **2021**, *6*, 33−40.

(40) Nwabara, U. O.; Hernandez, A. D.; Henckel, D. A.; Chen, X.; Cofell, E. R.; De-Heer, M. P.; Verma, S.; Gewirth, A. A.; Kenis, P. J. A. Binder-Focused Approaches to Improve the Stability of Cathodes for CO_2 Electroreduction. *ACS Appl. Energy Mater.* **2021**, *4*, 5175−5186.

(41) Hernandez-Aldave, S.; Andreoli, E. Fundamentals of Gas Diffusion Electrodes and Electrolysers for Carbon Dioxide Utilisation: Challenges and Opportunities. *Catalysts* **2020**, *10*, 713.

(42) Sassenburg, M.; Kelly, M.; Subramanian, S.; Smith, W. A.; Burdyny, T. Zero-Gap Electrochemical CO_2 Reduction Cells: Challenges and Operational Strategies for Prevention of Salt Precipitation. *ACS Energy Lett.* **2023**, *8*, 321−331.

(43) Leonard, M. E.; Clarke, L. E.; Forner-Cuenca, A.; Brown, S. M.; Brushett, F. R. Investigating Electrode Flooding in a Flowing Electrolyte, Gas-Fed Carbon Dioxide Electrolyzer. *ChemSusChem* **2020**, *13*, 400−411.

(44) Leonard, M. E.; Orella, M. J.; Aiello, N.; Román-Leshkov, Y.; Forner-Cuenca, A.; Brushett, F. R. Editors' Choice—Flooded by Success: On the Role of Electrode Wettability in CO_2 Electrolyzers that Generate Liquid Products. *J. Electrochem. Soc.* **2020**, *167*, 124521.

(45) Cofell, E. R.; Nwabara, U. O.; Bhargava, S. S.; Henckel, D. E.; Kenis, P. J. A. Investigation of Electrolyte-Dependent Carbonate Formation on Gas Diffusion Electrodes for CO_2 Electrolysis. *ACS Appl. Mater. Interfaces* **2021**, *13*, 15132−15142.

(46) Disch, J.; Bohn, L.; Koch, S.; Schulz, M.; Han, Y.; Tengattini, A.; Helfen, L.; Breitwieser, M.; Vierrath, S. High-resolution neutron imaging of salt precipitation and water transport in zero-gap CO_2 electrolysis. *Nat. Commun.* **2022**, *13*, 6099.

(47) Kong, Y.; Hu, H.; Liu, M.; Hou, Y.; Kolivoška, V.; Vesztergom, S.; Broekmann, P. Visualisation and quantification of flooding phenomena in gas diffusion electrodes used for electrochemical CO_2 reduction: A combined EDX/ICP-MS approach. *J. Catal.* **2022**, *408*, 1−8.

(48) Kong, Y.; Liu, M.; Hu, H.; Hou, Y.; Vesztergom, S.; Gálvez-Vázquez, M. d. J.; Zelocualtecatl Montiel, I.; Kolivoška, V.; Broekmann, P. Cracks as Efficient Tools to Mitigate Flooding in Gas Diffusion Electrodes Used for the Electrochemical Reduction of Carbon Dioxide. *Small Methods* **2022**, *6*, 2200369.

(49) Chen, L. D. Cations play an essential role in CO2 reduction. *Nat. Catal.* **2021**, *4*, 641−642.

(50) Endrödi, B.; Samu, A.; Kecsenovity, E.; Halmágyi, T.; Sebök, D.; Janáky, C. Operando cathode activation with alkali metal cations for high current density operation of water-fed zero-gap carbon dioxide electrolysers. *Nat. Energy* **2021**, *6*, 439−448.

(51) De Mot, B.; Ramdin, M.; Hereijgers, J.; Vlugt, T. J. H.; Breugelmans, T. Direct Water Injection in Catholyte-Free Zero-Gap Carbon Dioxide Electrolyzers. *ChemElectroChem.* **2020**, *7*, 3839−3843.

(52) Xu, Y.; Edwards, J. P.; Liu, S.; Miao, R. K.; Huang, J. E.; Gabardo, C. M.; O'Brien, C. P.; Li, J.; Sargent, E. H.; Sinton, D. Self-Cleaning CO_2 Reduction Systems: Unsteady Electrochemical Forcing Enables Stability. *ACS Energy Lett.* **2021**, *6*, 809−815.

(53) Wu, Y.; Charlesworth, L.; Maglaya, I.; Idros, M. N.; Li, M.; Burdyny, T.; Wang, G.; Rufford, T. E. Mitigating Electrolyte Flooding

for Electrochemical CO_2 Reduction via Infiltration of Hydrophobic Particles in a Gas Diffusion Layer. *ACS Energy Lett.* **2022**, 7, 2884−2892.

(54) Baumgartner, L. M.; Koopman, C. I.; Forner-Cuenca, A.; Vermaas, D. A. When Flooding Is Not Catastrophic-Woven Gas Diffusion Electrodes Enable Stable $CO_2$2 Electrolysis. *ACS Appl. Energy Mater.* **2022**, 5, 15125−15135.

(55) McCallum, C.; Gabardo, C. M.; O'Brien, C. P.; Edwards, J. P.; Wicks, J.; Xu, Y.; Sargent, E. H.; Sinton, D. Reducing the crossover of carbonate and liquid products during carbon dioxide electroreduction. *Cell Reports Phys. Sci.* **2021**, 2, 100522.

(56) Bondue, C. J.; Graf, M.; Goyal, A.; Koper, M. T. M. Suppression of Hydrogen Evolution in Acidic Electrolytes by Electrochemical CO_2 Reduction. *J. Am. Chem. Soc.* **2021**, 143, 279−285.

(57) Hori, Y. *Modern Aspects of Electrochemistry*; Springer New York: New York, NY, 2008; Vol. 42, pp 89−189. DOI: 10.1007/978-0-387-49489-0_3

(58) Huang, J. E.; et al. CO_2 electrolysis to multicarbon products in strong acid. *Science* **2021**, 372, 1074−1078.

(59) Xie, Y.; et al. High carbon utilization in CO_2 reduction to multi-carbon products in acidic media. *Nat. Catal.* **2022**, 5, 564−570.

(60) Pan, B.; Fan, J.; Zhang, J.; Luo, Y.; Shen, C.; Wang, C.; Wang, Y.; Li, Y. Close to 90% Single-Pass Conversion Efficiency for CO_2 Electroreduction in an Acid-Fed Membrane Electrode Assembly. *ACS Energy Lett.* **2022**, 7, 4224−4231.

(61) Monteiro, M. C. O.; Dattila, F.; López, N.; Koper, M. T. M. The Role of Cation Acidity on the Competition between Hydrogen Evolution and CO_2 Reduction on Gold Electrodes. *J. Am. Chem. Soc.* **2022**, 144, 1589−1602.

(62) Singh, M. R.; Kwon, Y.; Lum, Y.; Ager, J. W.; Bell, A. T. Hydrolysis of Electrolyte Cations Enhances the Electrochemical Reduction of CO_2 over Ag and Cu. *J. Am. Chem. Soc.* **2016**, 138, 13006−13012.

(63) Monteiro, M. C. O.; Dattila, F.; Hagedoorn, B.; García-Muelas, R.; López, N.; Koper, M. T. M. Absence of CO_2 electroreduction on copper, gold and silver electrodes without metal cations in solution. *Nat. Catal.* **2021**, 4, 654−662.

(64) Monteiro, M. C. O.; Philips, M. F.; Schouten, K. J. P.; Koper, M. T. M. Efficiency and selectivity of CO2 reduction to CO on gold gas diffusion electrodes in acidic media. *Nat. Commun.* **2021**, 12, 4943.

(65) Monteiro, M. C.; Koper, M. T. Measuring local pH in electrochemistry. *Curr. Opin. Electrochem.* **2021**, 25, 100649.

(66) Monteiro, M. C. O.; Dieckhöfer, S.; Bobrowski, T.; Quast, T.; Pavesi, D.; Koper, M. T. M.; Schuhmann, W. Probing the local activity of CO_2 reduction on gold gas diffusion electrodes: effect of the catalyst loading and CO 2 pressure. *Chem. Sci.* **2021**, 12, 15682−15690.

(67) Marcandalli, G.; Goyal, A.; Koper, M. T. M. Electrolyte Effects on the Faradaic Efficiency of CO 2 Reduction to CO on a Gold Electrode. *ACS Catal.* **2021**, 11, 4936−4945.

(68) Marcandalli, G.; Monteiro, M. C. O.; Goyal, A.; Koper, M. T. M. Electrolyte Effects on CO 2 Electrochemical Reduction to CO. *Acc. Chem. Res.* **2022**, 55, 1900−1911.

(69) Marcandalli, G.; Boterman, K.; Koper, M. T. Understanding hydrogen evolution reaction in bicarbonate buffer. *J. Catal.* **2022**, 405, 346−354.

(70) Ramdin, M.; Morrison, A. R. T.; de Groen, M.; van Haperen, R.; de Kler, R.; van den Broeke, L. J. P.; Trusler, J. P. M.; de Jong, W.; Vlugt, T. J. H. High Pressure Electrochemical Reduction of CO_2 to Formic Acid/Formate: A Comparison between Bipolar Membranes and Cation Exchange Membranes. *Ind. Eng. Chem. Res.* **2019**, 58, 1834−1847.

(71) Sheng, X.; Ge, W.; Jiang, H.; Li, C. Engineering the Ni-N-C Catalyst Microenvironment Enabling CO_2 Electroreduction with Nearly 100% CO Selectivity in Acid. *Adv. Mater.* **2022**, 34, 2201295.

(72) Li, H.; Li, H.; Wei, P.; Wang, Y.; Zang, Y.; Gao, D.; Wang, G.; Bao, X. Tailoring acidic microenvironments for carbon-efficient CO_2

electrolysis over a Ni-N-C catalyst in a membrane electrode assembly electrolyzer. *Energy Environ. Sci.* **2023**, 16, 1502.

(73) Zhao, Y.; et al. Conversion of CO_2 to multicarbon products in strong acid by controlling the catalyst microenvironment. *Nat. Synth.* **2023**. DOI: 10.1038/s44160-022-00234-x

(74) Chatti, M.; Gardiner, J. L.; Fournier, M.; Johannessen, B.; Williams, T.; Gengenbach, T. R.; Pai, N.; Nguyen, C.; MacFarlane, D. R.; Hocking, R. K.; Simonov, A. N. Intrinsically stable in situ generated electrocatalyst for long-term oxidation of acidic water at up to 80 °C. *Nat. Catal.* **2019**, 2, 457−465.

(75) Yang, K.; Li, M.; Subramanian, S.; Blommaert, M. A.; Smith, W. A.; Burdyny, T. Cation-Driven Increases of CO_2 Utilization in a Bipolar Membrane Electrode Assembly for CO_2 Electrolysis. *ACS Energy Lett.* **2021**, 6, 4291−4298.

(76) Salvatore, D. A.; Weekes, D. M.; He, J.; Dettelbach, K. E.; Li, Y. C.; Mallouk, T. E.; Berlinguette, C. P. Electrolysis of Gaseous CO_2 to CO in a Flow Cell with a Bipolar Membrane. *ACS Energy Lett.* **2018**, 3, 149−154.

(77) Yan, Z.; Hitt, J. L.; Zeng, Z.; Hickner, M. A.; Mallouk, T. E. Improving the efficiency of CO_2 electrolysis by using a bipolar membrane with a weak-acid cation exchange layer. *Nat. Chem.* **2021**, 13, 33−40.

(78) Xie, K.; Miao, R. K.; Ozden, A.; Liu, S.; Chen, Z.; Dinh, C.-T.; Huang, J. E.; Xu, Q.; Gabardo, C. M.; Lee, G.; Edwards, J. P.; O'Brien, C. P.; Boettcher, S. W.; Sinton, D.; Sargent, E. H. Bipolar membrane electrolyzers enable high single-pass CO_2 electroreduction to multicarbon products. *Nat. Commun.* **2022**, 13, 3609.

(79) Patru, A.; Binninger, T.; Pribyl, B.; Schmidt, T. J. Design Principles of Bipolar Electrochemical Co-Electrolysis Cells for Efficient Reduction of Carbon Dioxide from Gas Phase at Low Temperature. *J. Electrochem. Soc.* **2019**, 166, F34−F43.

(80) Zhang, T.; Bui, J. C.; Li, Z.; Bell, A. T.; Weber, A. Z.; Wu, J. Highly selective and productive reduction of carbon dioxide to multicarbon products via in situ CO management using segmented tandem electrodes. *Nat. Catal.* **2022**, 5, 202−211.

(81) Gurudayal; Perone, D.; Malani, S.; Lum, Y.; Haussener, S.; Ager, J. W. Sequential Cascade Electrocatalytic Conversion of Carbon Dioxide to C−C Coupled Products. *ACS Appl. Energy Mater.* **2019**, 2, 4551−4559.

(82) Lum, Y.; Ager, J. W. Sequential catalysis controls selectivity in electrochemical CO 2 reduction on Cu. *Energy Environ. Sci.* **2018**, 11, 2935−2944.

(83) Jouny, M.; Hutchings, G. S.; Jiao, F. Carbon monoxide electroreduction as an emerging platform for carbon utilization. *Nat. Catal.* **2019**, 2, 1062−1070.

(84) Hauch, A.; Küngas, R.; Blennow, P.; Hansen, A. B.; Hansen, J. B.; Mathiesen, B. V.; Mogensen, M. B. Recent advances in solid oxide cell technology for electrolysis. *Science* **2020**, 370, eaba6118.

(85) Küngas, R. Review—Electrochemical CO_2 Reduction for CO Production: Comparison of Low- and High-Temperature Electrolysis Technologies. *J. Electrochem. Soc.* **2020**, 167, 044508.

(86) Ozden, A.; Wang, Y.; Li, F.; Luo, M.; Sisler, J.; Thevenon, A.; Rosas-Hernández, A.; Burdyny, T.; Lum, Y.; Yadegari, H.; Agapie, T.; Peters, J. C.; Sargent, E. H.; Sinton, D. Cascade CO_2 electroreduction enables efficient carbonate-free production of ethylene. *Joule* **2021**, 5, 706−719.

(87) Sisler, J.; Khan, S.; Ip, A. H.; Schreiber, M. W.; Jaffer, S. A.; Bobicki, E. R.; Dinh, C.-T.; Sargent, E. H. Ethylene Electrosynthesis: A Comparative Techno-economic Analysis of Alkaline vs Membrane Electrode Assembly vs CO_2-CO-C_2H_4 Tandems. *ACS Energy Lett.* **2021**, 6, 997−1002.

(88) Dunwell, M.; Lu, Q.; Heyes, J. M.; Rosen, J.; Chen, J. G.; Yan, Y.; Jiao, F.; Xu, B. The Central Role of Bicarbonate in the Electrochemical Reduction of Carbon Dioxide on Gold. *J. Am. Chem. Soc.* **2017**, 139, 3774−3783.

(89) Li, T.; Lees, E. W.; Goldman, M.; Salvatore, D. A.; Weekes, D. M.; Berlinguette, C. P. Electrolytic Conversion of Bicarbonate into CO in a Flow Cell. *Joule* **2019**, 3, 1487−1497.

(90) Li, T.; Lees, E. W.; Zhang, Z.; Berlinguette, C. P. Conversion of Bicarbonate to Formate in an Electrochemical Flow Reactor. *ACS Energy Lett.* **2020**, *5*, 2624−2630.

(91) Lees, E. W.; Liu, A.; Bui, J. C.; Ren, S.; Weber, A. Z.; Berlinguette, C. P. Electrolytic Methane Production from Reactive Carbon Solutions. *ACS Energy Lett.* **2022**, *7*, 1712−1718.

(92) Zhang, Z.; Lees, E. W.; Ren, S.; Mowbray, B. A. W.; Huang, A.; Berlinguette, C. P. Conversion of Reactive Carbon Solutions into CO at Low Voltage and High Carbon Efficiency. *ACS Cent. Sci.* **2022**, *8*, 749−755.

(93) Gutiérrez-Sánchez, O.; de Mot, B.; Bulut, M.; Pant, D.; Breugelmans, T. Engineering Aspects for the Design of a Bicarbonate Zero-Gap Flow Electrolyzer for the Conversion of CO_2 to Formate. *ACS Appl. Mater. Interfaces* **2022**, *14*, 30760−30771.

(94) Li, Y. C.; Lee, G.; Yuan, T.; Wang, Y.; Nam, D.-H.; Wang, Z.; García de Arquer, F. P.; Lum, Y.; Dinh, C.-T.; Voznyy, O.; Sargent, E. H. CO_2 Electroreduction from Carbonate Electrolyte. *ACS Energy Lett.* **2019**, *4*, 1427−1431.

(95) Xiao, Y. C.; et al. Direct carbonate electrolysis into pure syngas. *EES Catal.* **2023**, *1*, 54−61.

(96) Gutiérrez-Sánchez, O.; de Mot, B.; Daems, N.; Bulut, M.; Vaes, J.; Pant, D.; Breugelmans, T. Electrochemical Conversion of CO_2 from Direct Air Capture Solutions. *Energy Fuels* **2022**, *36*, 13115−13123.

(97) Lee, G.; Li, Y. C.; Kim, J.-Y.; Peng, T.; Nam, D.-H.; Sedighian Rasouli, A.; Li, F.; Luo, M.; Ip, A. H.; Joo, Y.-C.; Sargent, E. H. Electrochemical upgrade of CO_2 from amine capture solution. *Nat. Energy* **2021**, *6*, 46−53.

(98) Liu, H.; Chen, Y.; Lee, J.; Gu, S.; Li, W. Ammonia-Mediated CO_2 Capture and Direct Electroreduction to Formate. *ACS Energy Lett.* **2022**, *7*, 4483−4489.

(99) Sanz-Pérez, E. S.; Murdock, C. R.; Didas, S. A.; Jones, C. W. Direct Capture of CO_2 from Ambient Air. *Chem. Rev.* **2016**, *116*, 11840−11876.

(100) Lv, B.; Guo, B.; Zhou, Z.; Jing, G. Mechanisms of CO_2 Capture into Monoethanolamine Solution with Different CO_2 Loading during the Absorption/Desorption Processes. *Environ. Sci. Technol.* **2015**, *49*, 10728−10735.

(101) Idris, Z.; Jens, K. J.; Eimer, D. A. Speciation of MEA-CO_2 Adducts at Equilibrium Using Raman Spectroscopy. *Energy Procedia* **2014**, *63*, 1424−1431.

(102) Jerng, S. E.; Gallant, B. M. Electrochemical reduction of CO_2 in the captured state using aqueous or nonaqueous amines. *iScience* **2022**, *25*, 104558.

(103) Darde, V.; Thomsen, K.; van Well, W. J.; Stenby, E. H. Chilled ammonia process for CO_2 capture. *Int. J. Greenh. Gas Control* **2010**, *4*, 131−136.

(104) Darde, V.; van Well, W. J. M.; Stenby, E. H.; Thomsen, K. Modeling of Carbon Dioxide Absorption by Aqueous Ammonia Solutions Using the Extended UNIQUAC Model. *Ind. Eng. Chem. Res.* **2010**, *49*, 12663−12674.

(105) Rastegar, Z.; Ghaemi, A. CO_2 absorption into potassium hydroxide aqueous solution: experimental and modeling. *Heat Mass Transfer* **2022**, *58*, 365−381.

(106) Yang, H.; Kaczur, J. J.; Sajjad, S. D.; Masel, R. I. Electrochemical conversion of CO_2 to formic acid utilizing Sustainion™ membranes. *J. CO_2 Util.* **2017**, *20*, 208−217.

(107) Kim, J. Y. T.; Zhu, P.; Chen, F.-Y.; Wu, Z.-Y.; Cullen, D. A.; Wang, H. Recovering carbon losses in CO_2 electrolysis using a solid electrolyte reactor. *Nat. Catal.* **2022**, *5*, 288−299.

(108) Xie, K.; Ozden, A.; Miao, R. K.; Li, Y.; Sinton, D.; Sargent, E. H. Eliminating the need for anodic gas separation in CO_2 electroreduction systems via liquid-to-liquid anodic upgrading. *Nat. Commun.* **2022**, *13*, 3070.

(109) Liu, W.-J.; Xu, Z.; Zhao, D.; Pan, X.-Q.; Li, H.-C.; Hu, X.; Fan, Z.-Y.; Wang, W.-K.; Zhao, G.-H.; Jin, S.; Huber, G. W.; Yu, H.-Q. Efficient electrochemical production of glucaric acid and H_2 via glucose electrolysis. *Nat. Commun.* **2020**, *11*, 265.

(110) O'Brien, C. P.; Miao, R. K.; Liu, S.; Xu, Y.; Lee, G.; Robb, A.; Huang, J. E.; Xie, K.; Bertens, K.; Gabardo, C. M.; Edwards, J. P.; Dinh, C.-T.; Sargent, E. H.; Sinton, D. Single Pass CO_2 Conversion Exceeding 85% in the Electrosynthesis of Multicarbon Products via Local CO_2 Regeneration. *ACS Energy Lett.* **2021**, *6*, 2952−2959.

(111) Ramdin, M.; de Loos, T. W.; Vlugt, T. J. H. State-of-the-Art of CO_2 Capture with Ionic Liquids. *Ind. Eng. Chem. Res.* **2012**, *51*, 8149−8177.

(112) Tennyson, R. N.; Schaaf, R. P. Guidelines can help choose proper process for gas-treating plant. *Oil Gas J.* **1977**, *10* (1), 78−86.

(113) Bauer, F.; Persson, T.; Hulteberg, C.; Tamm, D. Biogas upgrading - technology overview, comparison and perspectives for the future. *Biofuels, Bioprod. Biorefining* **2013**, *7*, 499−511.

(114) Defu, L.; Jinqu, W. The Adsorption and Separation of Ethylene, Oxygen and Carbon Dioxide Gases on Molecular Sieves. *Adsorpt. Sci. Technol.* **2002**, *20*, 83−90.

(115) Jaschik, M.; Tanczyk, M.; Janusz-Cygan, A.; Wojdyła, A.; Warmuzinski, K. The separation of carbon dioxide from $CO_2/N_2/O_2$ mixtures using polyimide and polysulphone membranes. *Chem. Process Eng. - Inz. Chem. i Proces.* **2018**, *39*, 449−456.

(116) Ismail, A. F.; Chandra Khulbe, K.; Matsuura, T. *Gas Separation Membranes*; Springer International Publishing: Cham, Switzerland, 2015.

(117) Wu, F.; Argyle, M. D.; Dellenback, P. A.; Fan, M. Progress in O_2 separation for oxy-fuel combustion−A promising way for cost-effective CO_2 capture: A review. *Prog. Energy Combust. Sci.* **2018**, *67*, 188−205.

(118) Sarswat, A.; Sholl, D. S.; Lively, R. P. Achieving order of magnitude increases in CO_2 reduction reaction efficiency by product separations and recycling. *Sustain. Energy Fuels* **2022**, *6*, 4598−4604.

(119) Eisaman, M. D.; Alvarado, L.; Larner, D.; Wang, P.; Garg, B.; Littau, K. A. CO_2 separation using bipolar membrane electrodialysis. *Energy Environ. Sci.* **2011**, *4*, 1319−1328.

(120) Eisaman, M. D.; Alvarado, L.; Larner, D.; Wang, P.; Littau, K. A. CO_2 desorption using high-pressure bipolar membrane electrodialysis. *Energy Environ. Sci.* **2011**, *4*, 4031.

(121) Keith, D. W.; Holmes, G.; St Angelo, D.; Heidel, K. A Process for Capturing CO_2 from the Atmosphere. *Joule* **2018**, *2*, 1573−1594.

(122) Bains, P.; Psarras, P.; Wilcox, J. CO_2 capture from the industry sector. *Prog. Energy Combust. Sci.* **2017**, *63*, 146−172.

(123) Boor, V.; Frijns, J. E. B. M.; Perez-Gallent, E.; Giling, E.; Laitinen, A. T.; Goetheer, E. L. V.; van den Broeke, L. J. P.; Kortlever, R.; de Jong, W.; Moultos, O. A.; Vlugt, T. J. H.; Ramdin, M. Electrochemical Reduction of CO_2 to Oxalic Acid: Experiments, Process Modeling, and Economics. *Ind. Eng. Chem. Res.* **2022**, *61*, 14837−14846.

(124) Vass, Á.; Kormányos, A.; Kószó, Z.; Endrödi, B.; Janáky, C. Anode Catalysts in CO_2 Electrolysis: Challenges and Untapped Opportunities. *ACS Catal.* **2022**, *12*, 1037−1051.

(125) Vass, Á.; Endrödi, B.; Samu, G. F.; Balog, Á.; Kormányos, A.; Cherevko, S.; Janáky, C. Local Chemical Environment Governs Anode Processes in CO_2 Electrolyzers. *ACS Energy Lett.* **2021**, *6*, 3801−3808.

(126) Comerford, J. W.; Ingram, I. D. V.; North, M.; Wu, X. Sustainable metal-based catalysts for the synthesis of cyclic carbonates containing five-membered rings. *Green Chem.* **2015**, *17*, 1966−1987.

(127) Vennekoetter, J.-b.; Sengpiel, R.; Wessling, M. Beyond the catalyst: How electrode and reactor design determine the product spectrum during electrochemical CO_2 reduction. *Chem. Eng. J.* **2019**, *364*, 89−101.

(128) Yang, Y.; Li, F. Reactor design for electrochemical CO_2 conversion toward large-scale applications. *Curr. Opin. Green Sustain. Chem.* **2021**, *27*, 100419.

(129) Liang, S.; Altaf, N.; Huang, L.; Gao, Y.; Wang, Q. Electrolytic cell design for electrochemical CO_2 reduction. *J. $CO2$ Util.* **2020**, *35*, 90−105.

(130) Lin, R.; Guo, J.; Li, X.; Patel, P.; Seifitokaldani, A. Electrochemical Reactors for CO_2 Conversion. *Catalysts* **2020**, *10*, 473.

(131) Zhang, F.; Co, A. C. Direct Evidence of Local pH Change and the Role of Alkali Cation during CO_2 Electroreduction in Aqueous Media. *Angew. Chemie Int. Ed.* **2020**, *59*, 1674−1681.

(132) Clark, E. L.; Bell, A. T. Direct Observation of the Local Reaction Environment during the Electrochemical Reduction of CO_2. *J. Am. Chem. Soc.* **2018**, *140*, 7012−7020.

(133) Li, X.; Wang, H.-Y.; Yang, H.; Cai, W.; Liu, S.; Liu, B. In Situ/ Operando Characterization Techniques to Probe the Electrochemical Reactions for Energy Conversion. *Small Methods* **2018**, *2*, 1700395.

(134) Dieckhöfer, S.; Öhl, D.; Junqueira, J. R. C.; Quast, T.; Turek, T.; Schuhmann, W. Probing the Local Reaction Environment During High Turnover Carbon Dioxide Reduction with Ag-Based Gas Diffusion Electrodes. *Chem. - A Eur. J.* **2021**, *27*, 5906−5912.

(135) Zhang, Z.; Lees, E. W.; Habibzadeh, F.; Salvatore, D. A.; Ren, S.; Simpson, G. L.; Wheeler, D. G.; Liu, A.; Berlinguette, C. P. Porous metal electrodes enable efficient electrolysis of carbon capture solutions. *Energy Environ. Sci.* **2022**, *15*, 705−713.

(136) Fink, A. G.; Lees, E. W.; Gingras, J.; Madore, E.; Fradette, S.; Jaffer, S. A.; Goldman, M.; Dvorak, D. J.; Berlinguette, C. P. Electrolytic conversion of carbon capture solutions containing carbonic anhydrase. *J. Inorg. Biochem.* **2022**, *231*, 111782.

(137) Salvatore, D. A.; Gabardo, C. M.; Reyes, A.; O'Brien, C. P.; Holdcroft, S.; Pintauro, P.; Bahar, B.; Hickner, M.; Bae, C.; Sinton, D.; Sargent, E. H.; Berlinguette, C. P. Designing anion exchange membranes for CO_2 electrolysers. *Nat. Energy* **2021**, *6*, 339−348.

(138) Garg, S.; Giron Rodriguez, C. A.; Rufford, T. E.; Varcoe, J. R.; Seger, B. How membrane characteristics influence the performance of CO_2 and CO electrolysis. *Energy Environ. Sci.* **2022**, *15*, 4440−4469.

(139) Simons, R. Water splitting in ion exchange membranes. *Electrochim. Acta* **1985**, *30*, 275−282.

(140) Xing, Z.; Hu, L.; Ripatti, D. S.; Hu, X.; Feng, X. Enhancing carbon dioxide gas-diffusion electrolysis by creating a hydrophobic catalyst microenvironment. *Nat. Commun.* **2021**, *12*, 136.

(141) Weng, L.-C.; Bell, A. T.; Weber, A. Z. Modeling gas-diffusion electrodes for CO_2 reduction. *Phys. Chem. Chem. Phys.* **2018**, *20*, 16973−16984.

(142) Weng, L.-C.; Bell, A. T.; Weber, A. Z. Towards membrane-electrode assembly systems for CO_2 reduction: a modeling study. *Energy Environ. Sci.* **2019**, *12*, 1950−1968.

(143) Morrison, A. R. T.; van Beusekom, V.; Ramdin, M.; van den Broeke, L. J. P.; Vlugt, T. J. H.; de Jong, W. Modeling the Electrochemical Conversion of Carbon Dioxide to Formic Acid or Formate at Elevated Pressures. *J. Electrochem. Soc.* **2019**, *166*, E77−E86.

(144) Chinnathambi, S.; Ramdin, M.; Vlugt, T. J. H. Mass Transport Limitations in Electrochemical Conversion of CO_2 to Formic Acid at High Pressure. *Electrochem* **2022**, *3*, 549−569.

(145) Singh, M. R.; Goodpaster, J. D.; Weber, A. Z.; Head-Gordon, M.; Bell, A. T. Mechanistic insights into electrochemical reduction of CO_2 over Ag using density functional theory and transport models. *Proc. Natl. Acad. Sci. U. S. A.* **2017**, *114*, E8812−E8821.

(146) Kontogeorgis, G. M.; Schlaikjer, A.; Olsen, M. D.; Maribo-Mogensen, B.; Thomsen, K.; von Solms, N.; Liang, X. A Review of Electrolyte Equations of State with Emphasis on Those Based on Cubic and Cubic-Plus-Association (CPA) Models. *Int. J. Thermphys.* **2022**, *43*, 54.

(147) Novak, N.; Kontogeorgis, G. M.; Castier, M.; Economou, I. G. Extension of the eSAFT-VR Mie equation of state from aqueous to non-aqueous electrolyte solutions. *Fluid Phase Equilib.* **2023**, *56S*, 113618.

(148) de Hemptinne, J.-C.; Kontogeorgis, G. M.; Dohrn, R.; Economou, I. G.; ten Kate, A.; Kuitunen, S.; Fele Žilnik, L.; De Angelis, M. G.; Vesovic, V. A View on the Future of Applied Thermodynamics. *Ind. Eng. Chem. Res.* **2022**, *61*, 14664−14680.

(149) Habibi, P.; Rahbari, A.; Blazquez, S.; Vega, C.; Dey, P.; Vlugt, T. J. H.; Moultos, O. A. A New Force Field for OH^- for Computing Thermodynamic and Transport Properties of H_2 and O_2 in Aqueous NaOH and KOH Solutions. *J. Phys. Chem. B* **2022**, *126*, 9376−9387.

(150) Jamali, S. H.; Wolff, L.; Becker, T. M.; Bardow, A.; Vlugt, T. J. H.; Moultos, O. A. Finite-Size Effects of Binary Mutual Diffusion Coefficients from Molecular Dynamics. *J. Chem. Theory Comput.* **2018**, *14*, 2667−2677.

(151) Moultos, O. A.; Tsimpanogiannis, I. N.; Panagiotopoulos, A. Z.; Economou, I. G. Atomistic Molecular Dynamics Simulations of CO_2 Diffusivity in H_2O for a Wide Range of Temperatures and Pressures. *J. Phys. Chem. B* **2014**, *118*, 5532−5541.

(152) Naseri Boroujeni, S.; Maribo-Mogensen, B.; Liang, X.; Kontogeorgis, G. M. On the estimation of equivalent conductivity of electrolyte solutions: The effect of relative static permittivity and viscosity. *Fluid Phase Equilib.* **2023**, *567*, 113698.

(153) Jamali, S. H.; Wolff, L.; Becker, T. M.; de Groen, M.; Ramdin, M.; Hartkamp, R.; Bardow, A.; Vlugt, T. J. H.; Moultos, O. A. OCTP: ATool for On-the-Fly Calculation of Transport Properties of Fluids with the Order-n Algorithm in LAMMPS. *J. Chem. Inf. Model.* **2019**, *59*, 1290−1294.

(154) Rahbari, A.; Hens, R.; Nikolaidis, I. K.; Poursaeidesfahani, A.; Ramdin, M.; Economou, I. G.; Moultos, O. A.; Dubbeldam, D.; Vlugt, T. J. H. Computation of partial molar properties using continuous fractional component Monte Carlo. *Mol. Phys.* **2018**, *116*, 3331−3344.

(155) Wasik, D. O.; Polat, H. M.; Ramdin, M.; Moultos, O. A.; Calero, S.; Vlugt, T. J. H. Solubility of CO_2 in Aqueous Formic Acid Solutions and the Effect of NaCl Addition: A Molecular Simulation Study. *J. Phys. Chem. C* **2022**, *126*, 19424−19434.

(156) Dawass, N.; Langeveld, J.; Ramdin, M.; Pérez-Gallent, E.; Villanueva, A. A.; Giling, E. J. M.; Langerak, J.; van den Broeke, L. J. P.; Vlugt, T. J. H.; Moultos, O. A. Solubilities and Transport Properties of CO_2, Oxalic Acid, and Formic Acid in Mixed Solvents Composed of Deep Eutectic Solvents, Methanol, and Propylene Carbonate. *J. Phys. Chem. B* **2022**, *126*, 3572−3584.

(157) Rahbari, A.; Hartkamp, R.; Moultos, O. A.; Bos, A.; van den Broeke, L. J. P.; Ramdin, M.; Dubbeldam, D.; Lyulin, A. V.; Vlugt, T. J. H. Electro-osmotic Drag and Thermodynamic Properties of Water in Hydrated Nafion Membranes from Molecular Dynamics. *J. Phys. Chem. C* **2022**, *126*, 8121−8133.

(158) Lee, J.; Lee, W.; Ryu, K. H.; Park, J.; Lee, H.; Lee, J. H.; Park, K. T. Catholyte-free electroreduction of CO_2 for sustainable production of CO: concept, process development, techno-economic analysis, and CO_2 reduction assessment. *Green Chem.* **2021**, *23*, 2397−2410.

(159) Xia, C.; Zhu, P.; Jiang, Q.; Pan, Y.; Liang, W.; Stavitski, E.; Alshareef, H. N.; Wang, H. Continuous production of pure liquid fuel solutions via electrocatalytic CO_2 reduction using solid-electrolyte devices. *Nat. Energy* **2019**, *4*, 776−785.

(160) Fan, L.; Xia, C.; Zhu, P.; Lu, Y.; Wang, H. Electrochemical CO_2 reduction to high-concentration pure formic acid solutions in an all-solid-state reactor. *Nat. Commun.* **2020**, *11*, 3633.

(161) Rigdon, W. A.; Omasta, T. J.; Lewis, C.; Hickner, M. A.; Varcoe, J. R.; Renner, J. N.; Ayers, K. E.; Mustain, W. E. Carbonate Dynamics and Opportunities With Low Temperature, Anion Exchange Membrane-Based Electrochemical Carbon Dioxide Separators. *J. Electrochem. Energy Convers. Storage* **2017**, *14*, 1−8.

(162) Landon, J.; Kitchin, J. R. Electrochemical Concentration of Carbon Dioxide from an Oxygen/Carbon Dioxide Containing Gas Stream. *J. Electrochem. Soc.* **2010**, *157*, B1149.

(163) Rigdon, W. A.; Omasta, T. J.; Lewis, C. A.; Mustain, W. E. Reaction Dependent Transport of Carbonate and Bicarbonate through Anion Exchange Membranes in Electrolysis and Fuel Cell Operations. *ECS Meet. Abstr.* **2015**, *MA201502*, 967−967.

(164) Muroyama, A. P.; Beard, A.; Pribyl-Kranewitter, B.; Gubler, L. Separation of CO_2 from Dilute Gas Streams Using a Membrane Electrochemical Cell. *ACS ES&T Eng.* **2021**, *1*, 905−916.

(165) Pennline, H. W.; Granite, E. J.; Luebke, D. R.; Kitchin, J. R.; Landon, J.; Weiland, L. M. Separation of CO_2 from flue gas using electrochemical cells. *Fuel* **2010**, *89*, 1307−1314.

(166) Gurkan, B.; Su, X.; Klemm, A.; Kim, Y.; Mallikarjun Sharada, S.; Rodriguez-Katakura, A.; Kron, K. J. Perspective and challenges in

electrochemical approaches for reactive CO_2 separations. *iScience* **2021**, *24*, 103422.

(167) Seger, B.; Robert, M.; Jiao, F. Best practices for electrochemical reduction of carbon dioxide. *Nat. Sustain.* **2023**, *6*, 236−238.

☐ Recommended by ACS

Bridging Trans-Scale Electrode Engineering for Mass CO_2 Electrolysis

Guobin Wen, Zhongwei Chen, *et al.*

JULY 25, 2023
JACS AU

READ ☑

Techno-economic Assessment of CO_2 Electrolysis: How Interdependencies between Model Variables Propagate Across Different Modeling Scales

Isabell Bagemihl, J. Ruud van Ommen, *et al.*

JUNE 28, 2023
ACS SUSTAINABLE CHEMISTRY & ENGINEERING

READ ☑

Inhomogeneities in the Catholyte Channel Limit the Upscaling of CO_2 Flow Electrolysers

Joseph W. Blake, J. W. Haverkort, *et al.*

FEBRUARY 07, 2023
ACS SUSTAINABLE CHEMISTRY & ENGINEERING

READ ☑

Toward a Stackable CO_2-to-CO Electrolyzer Cell Design—Impact of Media Flow Optimization

Maximilian Quentmeier, Rüdiger-A. Eichel, *et al.*

JANUARY 04, 2023
ACS SUSTAINABLE CHEMISTRY & ENGINEERING

READ ☑

Get More Suggestions >